AD-A155 569 DISCOVERY OF A NONPROPAGATING HYDRODYNAMIC SOLITON(U) 1/2
CALIFORNIA UNIV LOS ANGELES DEPT OF PHYSICS J R WU
JUN 85 TR-43

UNCLASSIFIED F/G 20/4 NL

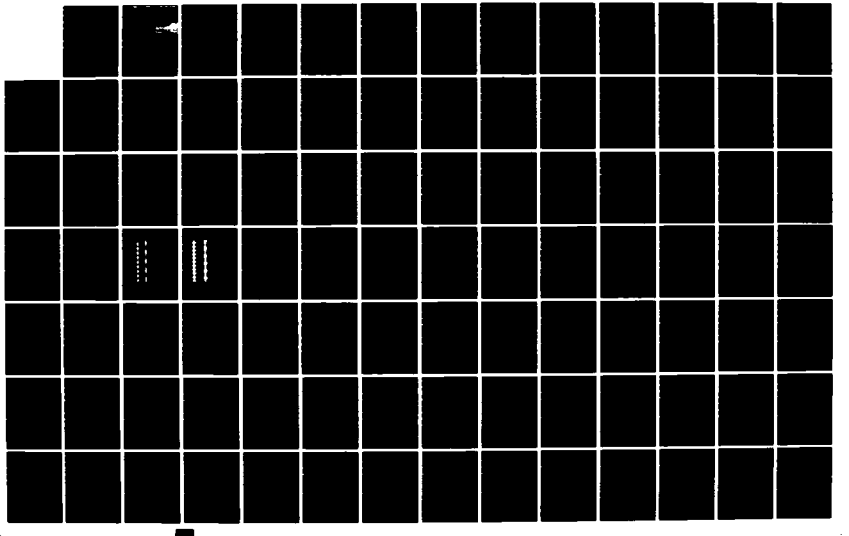

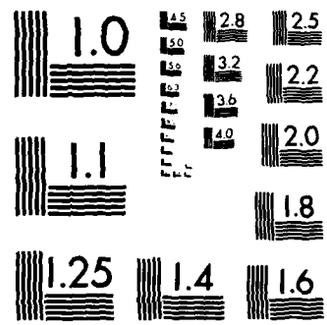

MICROCOPY RESOLUTION TEST CHART
NATIONAL BUREAU OF STANDARDS-1963-A

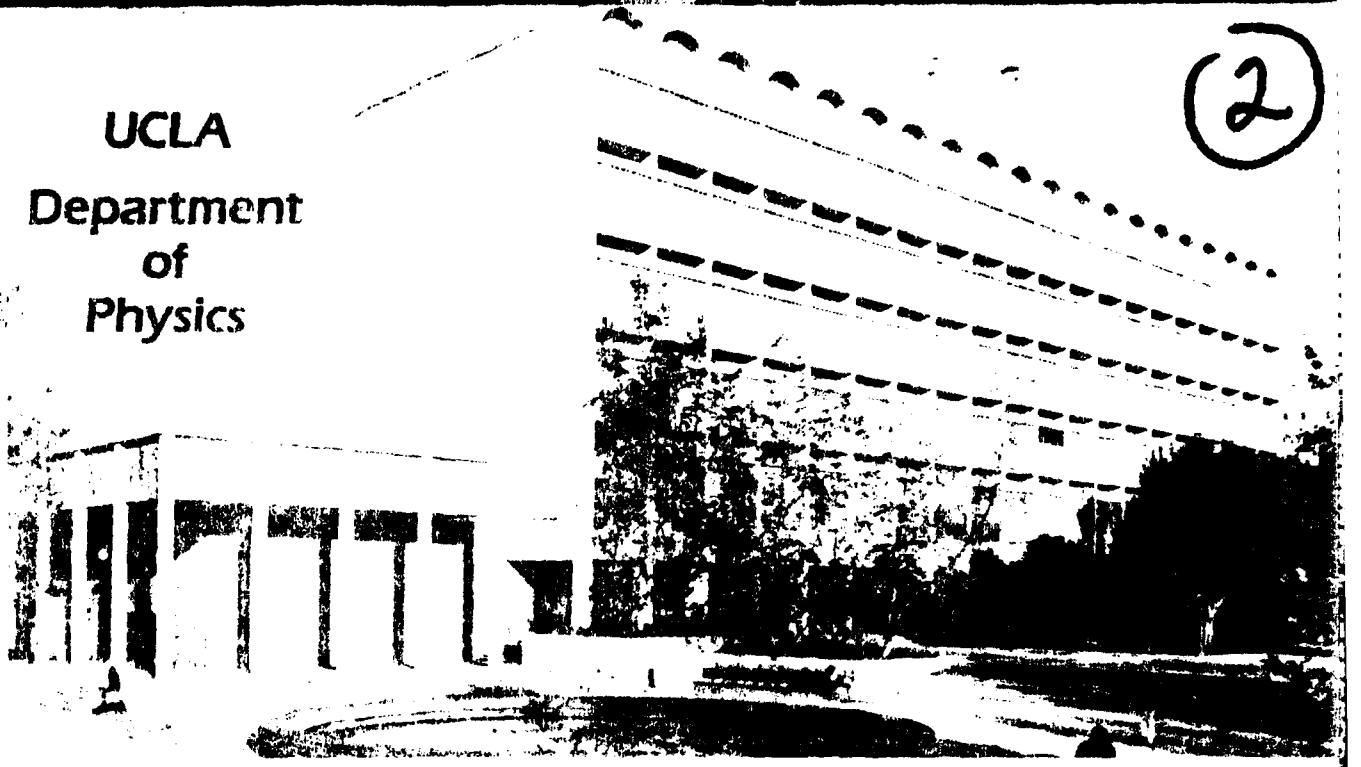

UCLA

Department

of

Physics

(2)

Discovery

of a Nonpropagating Hydrodynamic Soliton

by

Jun-Ru Wu

LOS ANGELES 90024

CALIFORNIA

TECHNICAL REPORT No. 43

June 1985

Submitted by

I. Rudnick, Project Director

Discovery

of a Nonpropagating Hydrodynamic Soliton

by

Jun-Ru Wu

office of Naval Research
Contract
4-484024-25895

Department of Physics
University of Californea
Los Angeles, Californea 90024

To my family

TABLE OF CONTENTS

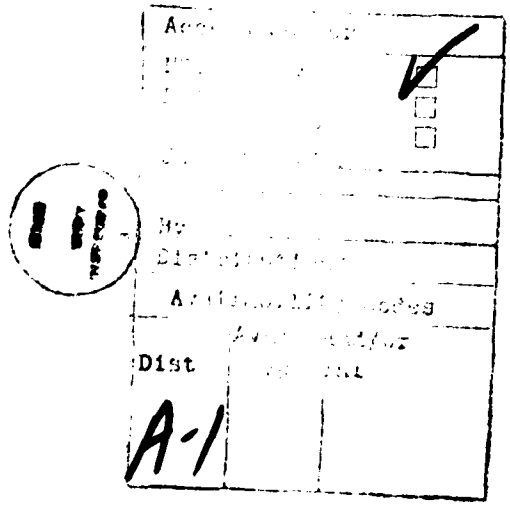

LIST OF FIGURES

FIGURES PAGE

FIGURES PAGE

FIGURES PAGE

FIGURES PAGE

ACKNOWLEDGEMENTS

I would like to acknowledge the incomparable contribution made by my thesis adviser Professor Isadore Rudnick, to this work and all aspects of my enjoyable 5 years at UCLA. It is his effort which made my Ph.D program at UCLA possible. It is his physical insight and expertise as an experimentalist which made everything in my experiment work.

I would like to express my sincere thanks to Professor Seth Putterman. It is from him I learned the fundamental theory of nonlinear physics. It is from him I share genuine friendship and inexhaustible stimulation of physics.

I would also like to thank Professor J. Rudnick, Professor F. Busse and Professor R. E. Kelly for being on my doctoral committee.

I am very grateful to Robert Keolian, Steve Baker and Dr. John Marcus. They actually taught me how to do a meaningful physical measurement when I just started. The nonlinear least square fitting computer program worked out by Steve Baker is very useful to my data analysis.

To all the friends, colleagues and classmates I owe a debt of gratitude for their useful and inspiring discussions,

suggestions and efforts on my behalf. Especially I would like to thank Andres Larraza, Bruce Denardo and Narbik Manukian for many successful and exciting nights we spent together in our study group, which has been proved to be very helpful to understand many difficult physical concepts.

I am grateful to Scott Hannahs for his computer consultations and help in many other ways.

I also wish to thank the other members of the Physics Department for their generous contributions: Jackie Payne for the graphics; Bud Knox and Pete Goodman in the machine shop; Barbara Cabot and Penny Lucky in the graduate affairs office; Liz Muldawer and Reta Watson, secretaries in our group.

ABSTRACT OF THE DISSERTATION

Discovery of a Nonpropagating Hydrodynamic Soliton

by

Jun-Ru Wu

Doctor of Philosophy in Physics

University of California, Los Angels, 1985

Professor Isadore Rudnick, Chairman

A new type water-surface-wave soliton, nonpropagating hydrodynamic soliton, has been discovered[1]. This is a self-trapped, highly localized and stationary transverse water-surface-wave excitation which appears in a rectangular cross section resonator continuously excited parametrically by vertical oscillation. (Fig. 1).

An experiment designed to create the soliton and the features of the soliton are described. The profiles of the soliton for various frequencies and amplitudes are measured. It is found that the profile of the soliton is accurately given by a hyperbolic secant function. The stability region that is the amplitude and frequency range of the drive in which individual soliton can be created without hysteresis is experimentally determined.

The interaction between two solitons has been investigated.

It is observed that an attractive force exists between two solitons with the same polarity and a repulsive force exists between two solitons with the opposite polarity. Under a certain range of drive frequencies and amplitudes, two solitons with the same polarity slowly oscillate through each other. The oscillation frequency has been measured.

The self-trapping mechanism of the soliton is studied. It is found that the necessary condition for creating the soliton is that our nonlinear dispersive system has an amplitude dependent resonant frequency of the transverse mode such that the higher the amplitude the lower the resonant frequency. The finite amplitude tuning curves of the rectangular cross section water-surface-wave have been determined for various liquid depths. The experimental results show that the direction of the bending of the tuning curve depends on the liquid depth. For a deep liquid it bends toward lower frequencies, and for a shallow liquid it bends toward higher frequencies. The so-called nonlinear coefficient is determined from these tuning curves. The cross-over from right leaning to left leaning was found to be in good agreement with the theoretical value calculated from the formula developed independently by J.Miles[2], and by A.Larraza and S. Putterman[3].

The soliton free decay rate is also measured. It is found that the soliton initially decays much faster than the corresponding linear transverse mode, but has the same rate in

the terminal decay.

CHAPTER I

INTRODUCTION

''....it has usually been thought that in a relativistic field theory, in order to have stationary bound states, quantum mechanics must be crucial. As we shall see, this turns out not to be the case. In a nonlinear field theory, with an appropriate amount of nonlinearity, stable bound states can exist on a classical, as well as quantum mechanical, level. Such bound states are called solitons.''

T.D.Lee[4]

A. AN HISTORICAL REVIEW OF SOLITONS IN A FLUID

The concept of a solitary wave was first introduced by a

Victorian engineer John Scott Russell in 1844 in his historical paper'' Report on Waves''(appendix A). He used the word ''solitary'' to characterize the robust, localized, and well defined ''heap'' of water which propagates along a narrow canal without change of form and diminution of speed[5]. Russell's observation appeared to contradict the famous contemporary scientist Airy's shallow water theory which predicts that a wave of finite amplitude cannot propagate without change of form[6].

The Airy paradox wasn't totally resolved until 1895 when Korteweg and deVries developed an equation for a water wave which includes both nonlinear and dispersive effects[7]. This equation has permanent solitary wave solutions(appendix B). It is now well known as the KdV equation, and provides a simple analytical foundation for the study of solitary waves.

A new impetus to this problem was generated by Fermi, Pasta, and Ulam's work in the early fifties[8]. They used the first large electronic computer, Maniac I, to investigate the time evolution of the energy of a weakly and nonlinearly coupled system of sixty four harmonic oscillators. They started with the case when the energy was initially concentrating in one of the modes. To their great surprise, the classical equipartition theorem, describing the thermal equilibrium , turned out to be incorrect. After some tens of thousands of cycles, the energy invariably returned almost completely to the original mode. This

is well known now as F.P.U. Recurrence , and is evidence that the development of such a collective mode is a general phenomenon. It occurs in the other fields of the physics, outside of hydrodynamics(appendix C).

In 1965 N. J. Zabusky and M. D. Kruskal found from their numerical simulation of the nonlinear discrete mass string problem that an intially sinusoidal profile would decompose into a series of interacting solitary waves and each one of them retained its identity after each interaction[9]. It is the first time that the term soliton was used to characterize this kind of solitary wave which has the property of emerging from the collision having the same shape and velocity with which it entered - a remarkable resemblance to the elastic interaction of particles.

Although the term soliton was originally applied only to the solitary waves of the KdV equation, there are now several nonlinear partial differential equations known to exhibit similar effects. Among them, especially for fluid solitons, the Nonlinear Schrodinger Equation (NLS) is a popular one[10]. In 1968 Zakharov predicted that the time evolution of weakly nonlinear deep-water-waves obeys NLS and three years later Zakharov and Shabat found the exact solution for the equation[11]. In 1975 Yuen and Lake[12] verified the prediction, and observed the so-called envelope soliton in a narrow water

tank(appendix D). The envelope soliton can be pictured as a quickly oscillating wave cut off by a smoothly modulating envelope (Fig.2). Until recently the KdV and envelope solitons were the only known solitary waves in fluids. Both of these solitons have to propagate at a non-zero group velocity determined by their amplitudes and shapes. They are also limited to motion in one dimension.

Recent theoretical efforts, as far as fluid mechanics is concerned, concentrate on extending the one dimensional classical soliton solution to higher dimensions[13].

B. AN INTRODUCTION TO THE NEWLY DISCOVERED NONPROPAGATING HYDRODYNAMIC SOLITON

The nonpropagating soliton was first observed in Professor I. Rudnick's laboratory in the summer of 1983 in a fluid trough driven sinusoidally and vertically from below so that all the fluid is caused to accelerate up and down equally. A localized surface pulse could be observed. The motion of the pulse appeared to be so stable and robust that it was immediately thought to be a soliton. Furthermore, since it could appear and be stationary anywhere along the length of the trough and sloshes back and forth across the width of the trough, more than one dimension is involved. It is fundamentally different from the other two types of soliton and is called a nonpropagating

hydrodynamic soliton.

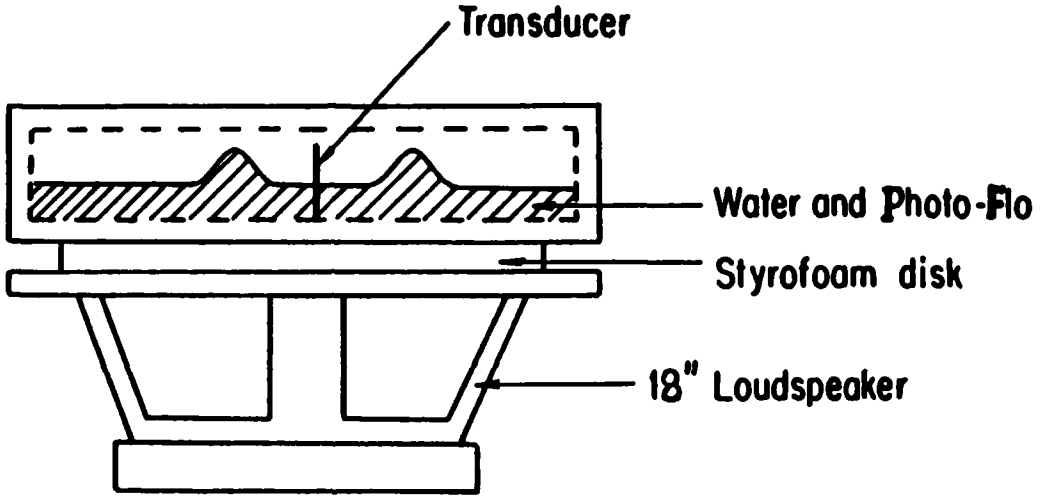

FIGURE 1. Schematic of a parametrically driven water trough.

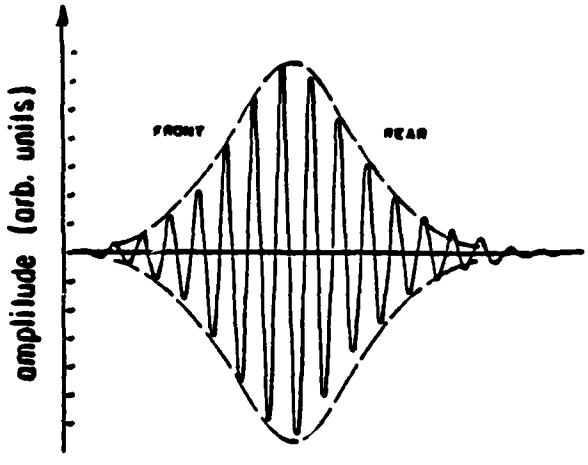

FIGURE 2. A plot of an envelope soliton.

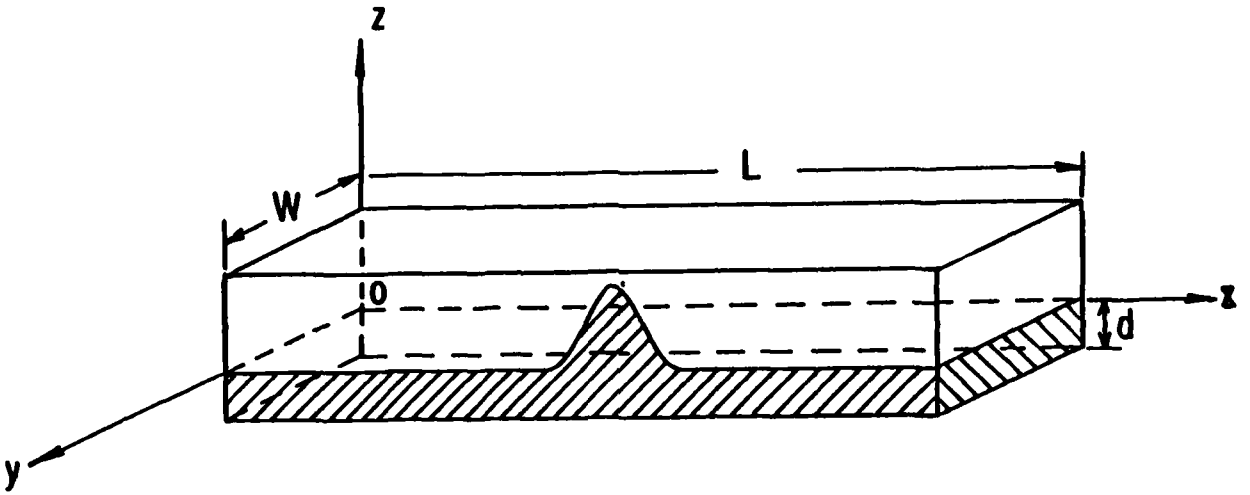

FIGURE 3. Schematic of a rectangular water-surface-wave resonator.

C. BRIEF REVIEW OF WAVEGUIDE THEORY

To understand the physics of a nonpropagating soliton, it is essential to review waveguide theory. Suppose the trough is very long so that it can be regarded as a waveguide with length coordinate x and width coordinate y (Fig.3). The depth of liquid, d, controls the surface wave phase velocity ,c, given by

$$c^2 = (g/k + \mu k/\rho)\tanh(kd) \qquad (1)$$

where k is the wave number, g is the acceleration of gravity, μ is the surface tention and ρ is the density of fluid. The surface displacement, z, is given by

$$z = a\cos(k_y y)\exp[i(k_x x \pm 2\pi\nu t)] \qquad (2)$$

where ν is frequency, $k_y W = q\pi$, W is the width of the trough, q = 0,1,2,3... and

$$k_x = (k^2 - k_y^2)^{\frac{1}{2}} = (2\pi/c)(\nu^2 - \nu_{cutoff}^2)^{\frac{1}{2}} \qquad (3)$$

$$\nu_{cutoff} = \frac{qc}{2W}. \qquad (4)$$

The case q = 0 is the plane wave mode, q = 1 has one velocity

component, v_y, antinode between the side walls, q = 2 has two, etc. The energy of the wave propagates with the group velocity, v_g, which can be calculated by

$$c_g = \frac{c}{v}\left(v^2 - v_{cutoff}^2 \right)^{\frac{1}{2}} \qquad (5)$$

If $v > v_{cutoff}$, k_x and c_g are real, energy propagates down the waveguide in a angle of $\theta = \cos^{-1}[1 - (v_{cutoff}/v)^2]^{\frac{1}{2}}$ with the x direction(Fig. 4). If $v < v_{cutoff}$ then k_x and c_g are imaginary. The amplitude of this particular mode decays exponentially down the waveguide, and energy will not propagate, but is instead totally reflected back. This is a so-called evanescent wave. For a finite waveguide of length L like our resonator,

$$z = a\cos(k_x x)\cos(k_y y)\cos(2\pi\nu t) \qquad (6)$$

where $k_x L = p\pi$ and $p = 0,1,2,3....$ Resonant frequencies are given by

$$\nu_{p,q} = (c/2)[(p/W)^2 + (q/L)^2]^{\frac{1}{2}}. \qquad (7)$$

The (0,1) mode is the equivalent of being the first cutoff for the infinite waveguide.

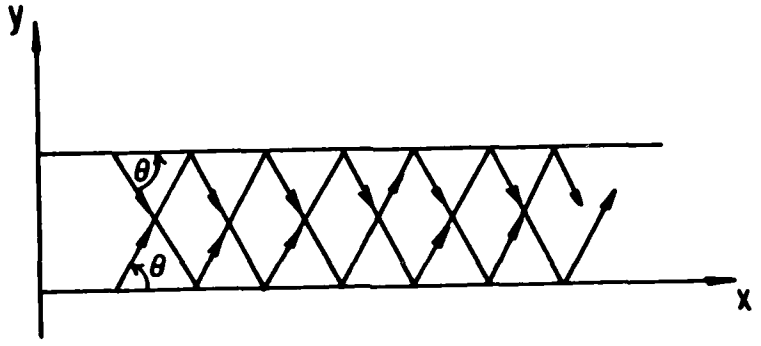

FIGURE 4. The (0,q) mode waves zigzag down the waveguide.

CHAPTER II

OBSERVATION OF A NONPROPAGATING SOLITON

'' You make experiments and I make theories. Do you know the difference? A theory is something nobody believes except the person who made it, while an experiment is something everybody believes except the person who made it.''

A. Einstein[14]

The apparatus for getting a nonpropagating soliton is quite simple. We use a Plexiglas (or glass) channel 38 cm long and 2.6 cm wide filled with still water (unless otherwise specified, the working liquid is still water) to a depth of 2 cm. Several drops of the wetting agent Kodak Photo-Flo are added to the water to minimize surface pinning effects at the walls. Waves are generated by placing the trough horizontally on a 18'' loudspeaker (or a vibration exciter, 4809, Bruel Kjaer) whose cone is driven at a frequency 2ν in the vertical direction. As

s.own by Eq.(7), there could be (p,q) modes appearing in the trough.

It is found that with this parametric excitation all low-lying (p,0) modes can be observed. When we parametrically excite the (0,1) mode, however, there is some degree of competition between various modes at the initial stage, then the sloshing motion in y direction corresponding to (0,1) mode developes and appears to be unstable. Finally the waves merge and focus themselves to one or more excitations highly localized in x-direction, sloshing in y-direction. Importance is attached to this self-focussing behavior. It is surprising and intriguing that while all parts of the trough are oscillated with equal amplitude, the vigorous wave motion occurs in a space of a few centimeters long while the rest of the water remains tranquil. The phase shift along the x-direction given by Eq.(2) for ν_{cutoff} = 5.1 hz and ν = 5.4 hz is 90° in a distance of 6 cm. Yet, within our resolution of 3°, we find no measurable phase difference between any two points of the disturbance. It is believed that the absence of a phase difference is of fundamental importance. The wave is not simply a waveguide mode occuring slighly above the cutoff frequency but a new type of nonpropagating solitary wave. As we proceed we shall see that it has properties usually associated with solitons.

Figure 5 and 6 are computer generated profiles of the

soliton based on measurements taken from photographs, when it is respectively at its peaks on the far side of the trough and on the near side of the trough. The wave frequency here is 5.1 hz and the peak amplitude is 2.1 cm.

Figs 7 - 10 contain plots of the heights z of the solitons as functions of x for various frequencies and the same amplitudes of the drive, when they are at their peaks on the walls. The points are experimental data and the curves are least square fits. From the plots, it is evident that our solitons have the following features.

The hyperbolic secant, a function which characterizes some solitons, fits our soliton profile in x direction very well. The amplitude of the nonpropagating soliton can be as high, or higher than the water depth.

The characteristic length, which is defined as the characteristic decay length at its wings, and the amplitude of the soliton are determined by the frequency of the excitation for the same amplitude driven system. They are interrelated in such a way that the higher the amplitude the shorter the characteristic length.

The frequency of the sloshing motion of the nonpropagating soliton is lower than ν_{cutoff} given by Eq. 4.

The dependence of z on y when the soliton is at its peak is found to be far from a cosine function which is linear solution

to the Laplace equation. A best-fit function is found to be an exponential function (Fig. 11).

It is found experimentally that one of the important feature of our soliton is that the velocity along the x-direction of the localized disturbance is a free parameter. It can be zero if the trough is accurately horizontal, which means the soliton maintains its initial x-position in the trough for the order of an hour or more. We hypothesize that this stability is due to pinning effects at the wall. The soliton, however, can be moved in various ways. One such way is to tilt the trough. For a slope of 0.05, for instance, the soliton slowly moves to the shallow end with an average speed of 0.05 cm/sec. It moves in response to gentle jets of air. It can also be nudged by rods of soft sponge plastic. Unwanted solitons are killed by stabbing them with such rods.

The stability range, defined as the range of the amplitudes and frequencies of the drive in which individual solitons are observed without hysteresis, were measured and found to be as shown by the dashed lines of Fig. 12. The eight full-line curves are equal-wave-response curves. The number on each is the peak height in centimeters of the soliton above the equilibrium level of the water. Note that at 0.7 and 2.1 cm the curves are so short that they are only represented by points. From the plot we see that for the same amplitude of drive, the lower the frequency

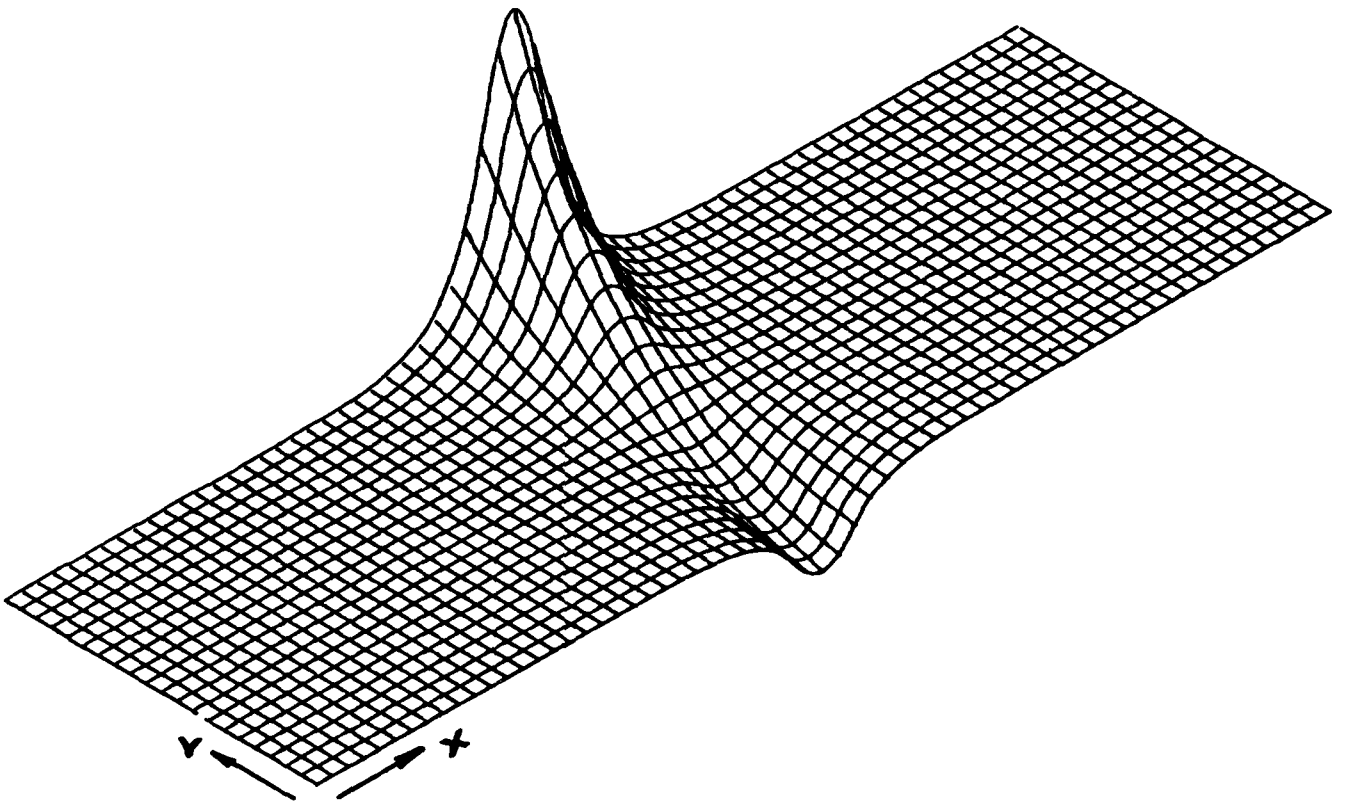

FIGURE 5 A plot of the profile of a nonpropagating hydrodynamic soliton when it is at its peak on the far side of the trough.

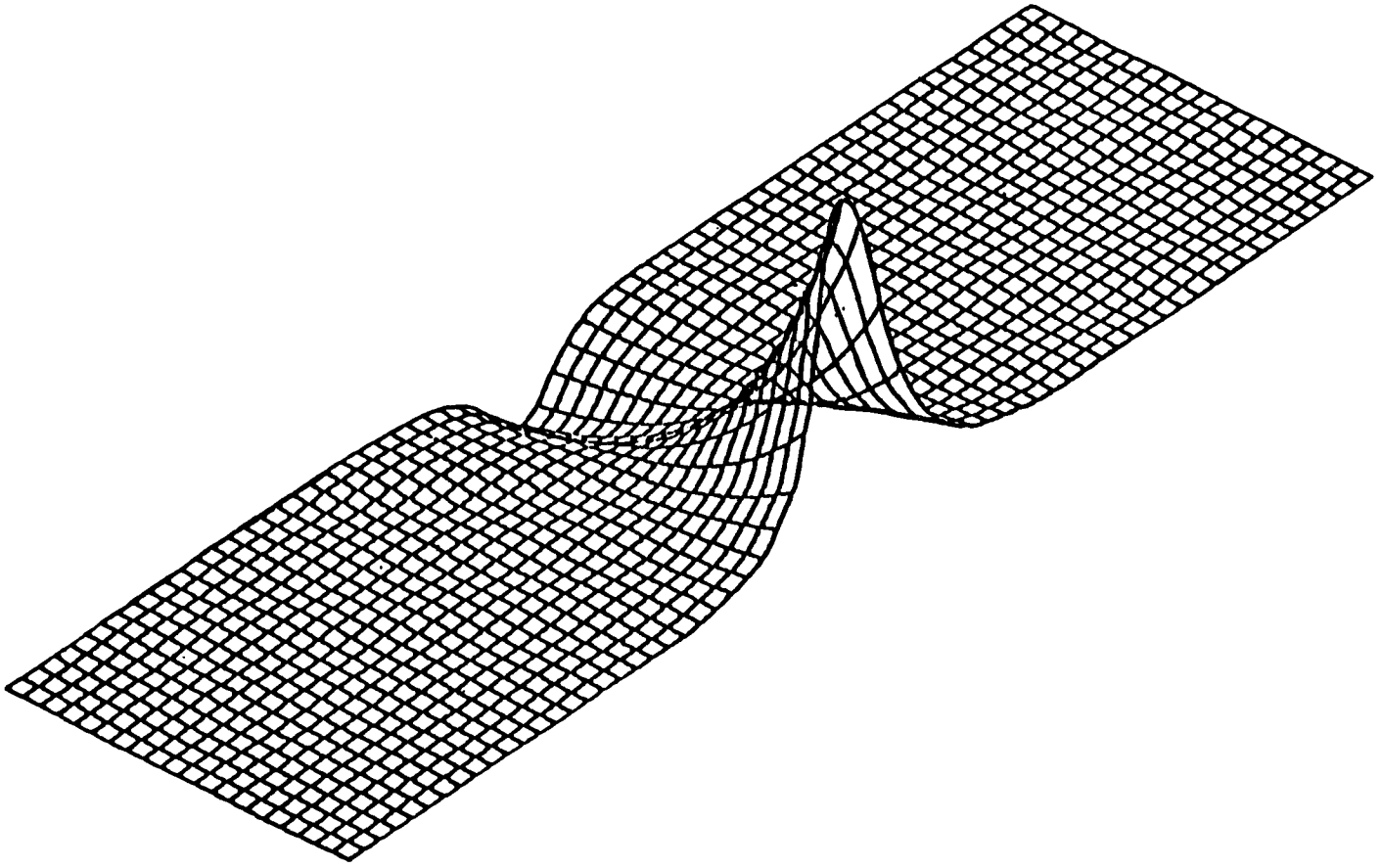

FIGURE 6 A plot of the same soliton when it is at its peak on the near side of the trough.

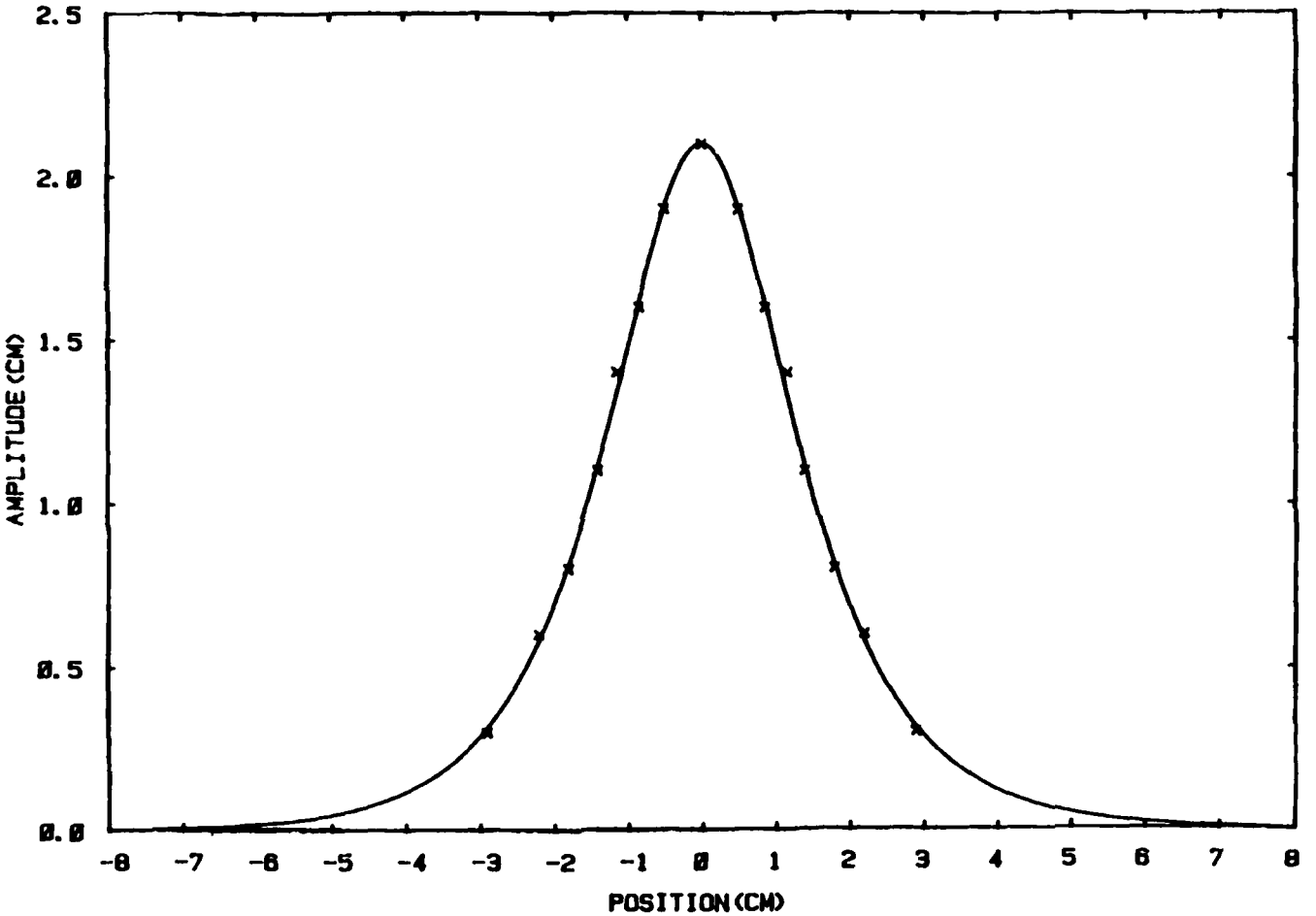

FIGURE 7. The profile of a soliton (f = 5.10 hz) as a function of x. The points are experimental data, and the solid curve is z = 2.1sech(0.89x) cm.

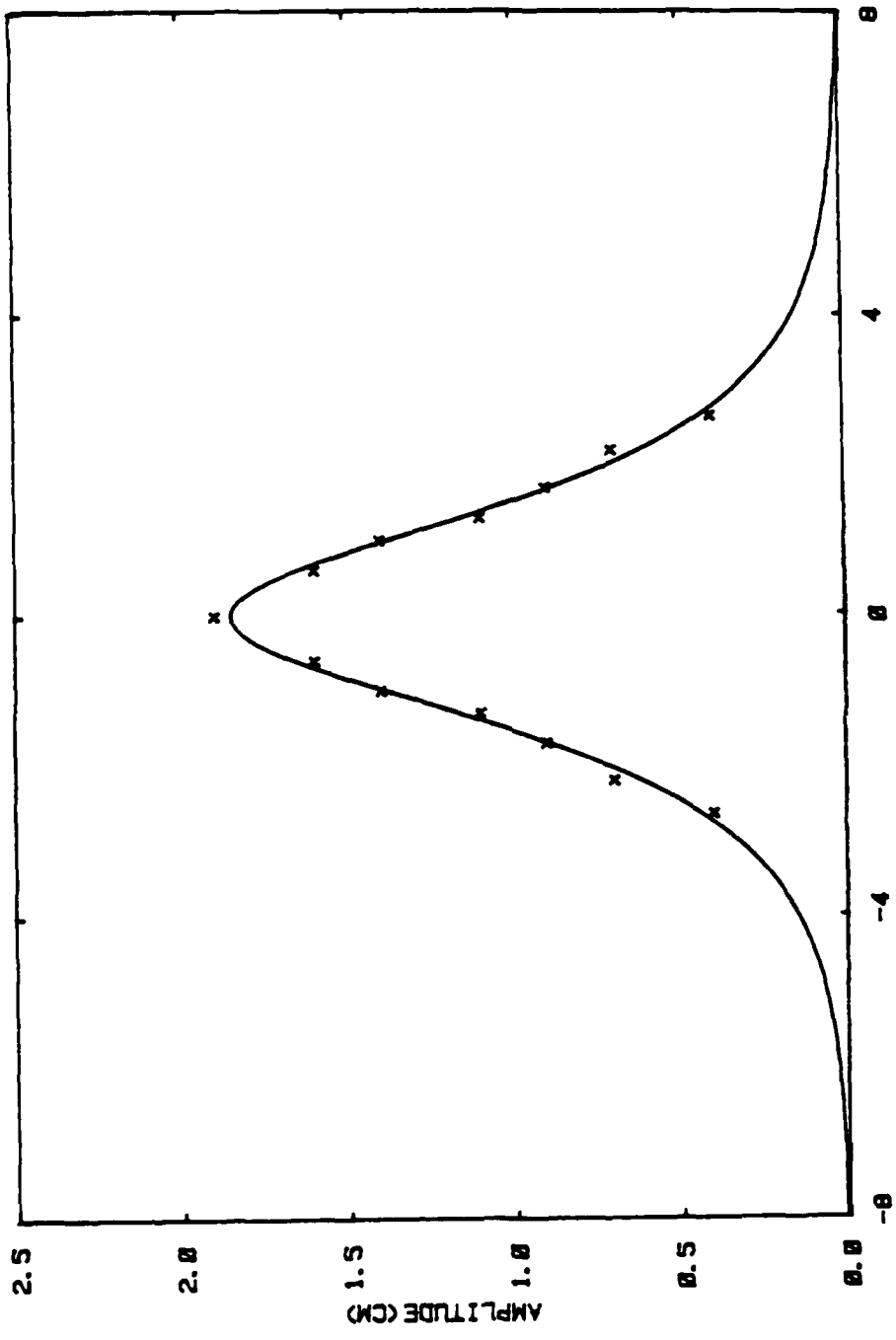

FIGURE 8. The profile of a soliton (f = 5.20 hz) as a function of x. The points are experimental data, and the solid curve is z = 1.85sech(0.80x) cm.

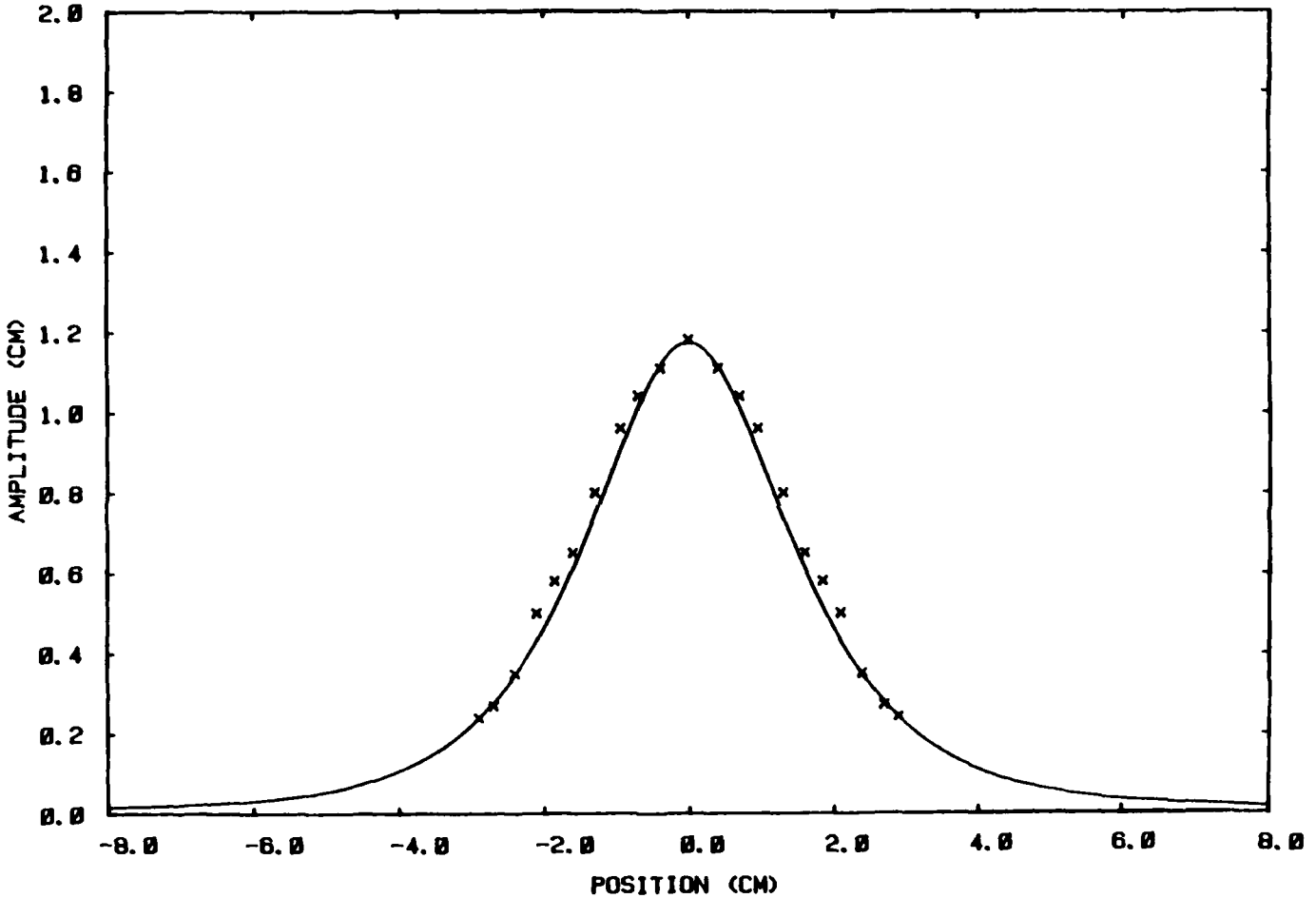

FIGURE 9. The profile of a soliton (f = 5.25 hz) as a function of x. The points are experimental data, and the solid curve is z = 1.16sech(0.80x) cm.

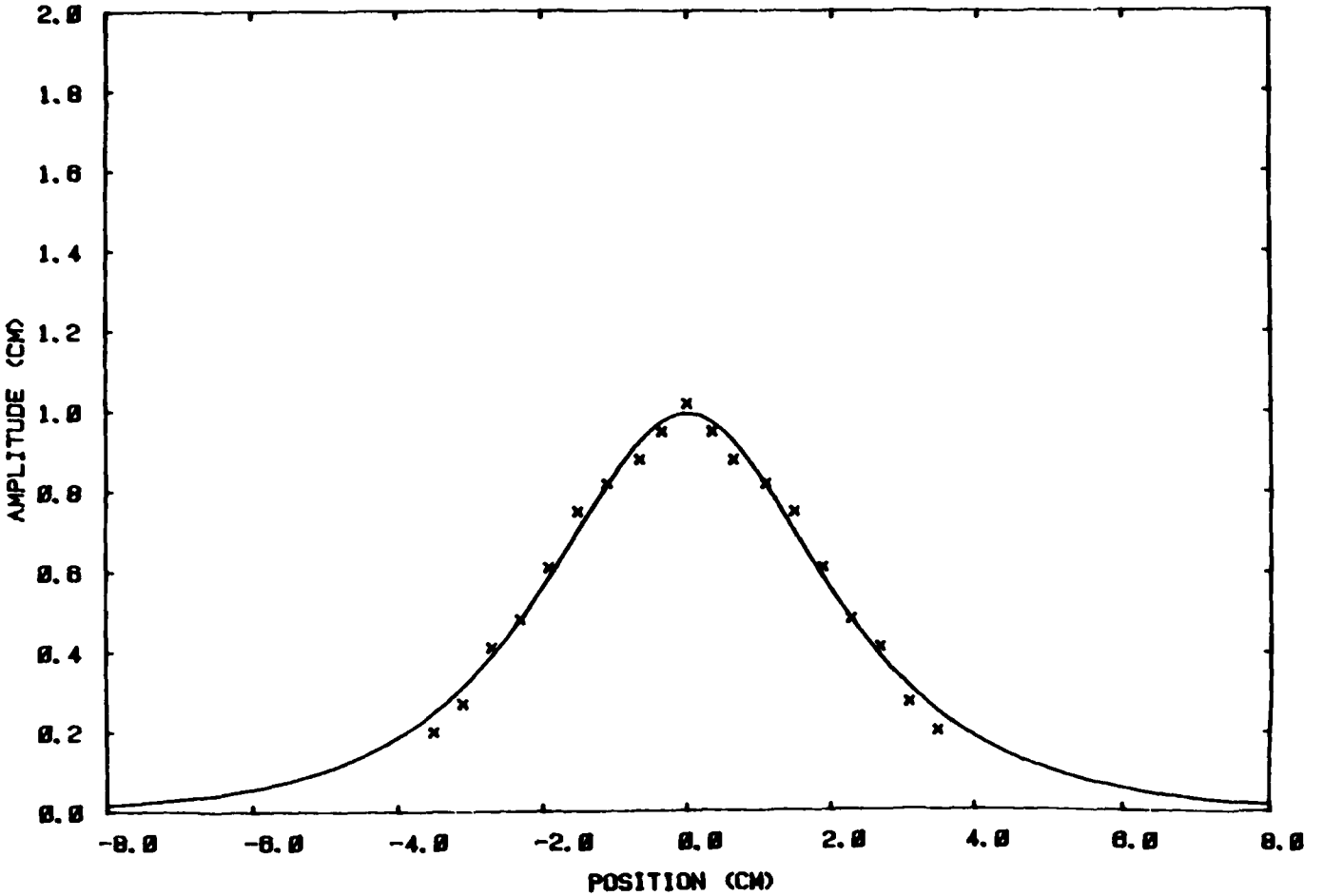

FIGURE 10. The profile of a soliton (f = 5.35 hz) as a function of x. The points are experimental data, and the solid curve is z = 0.995sech(0.59x) cm.

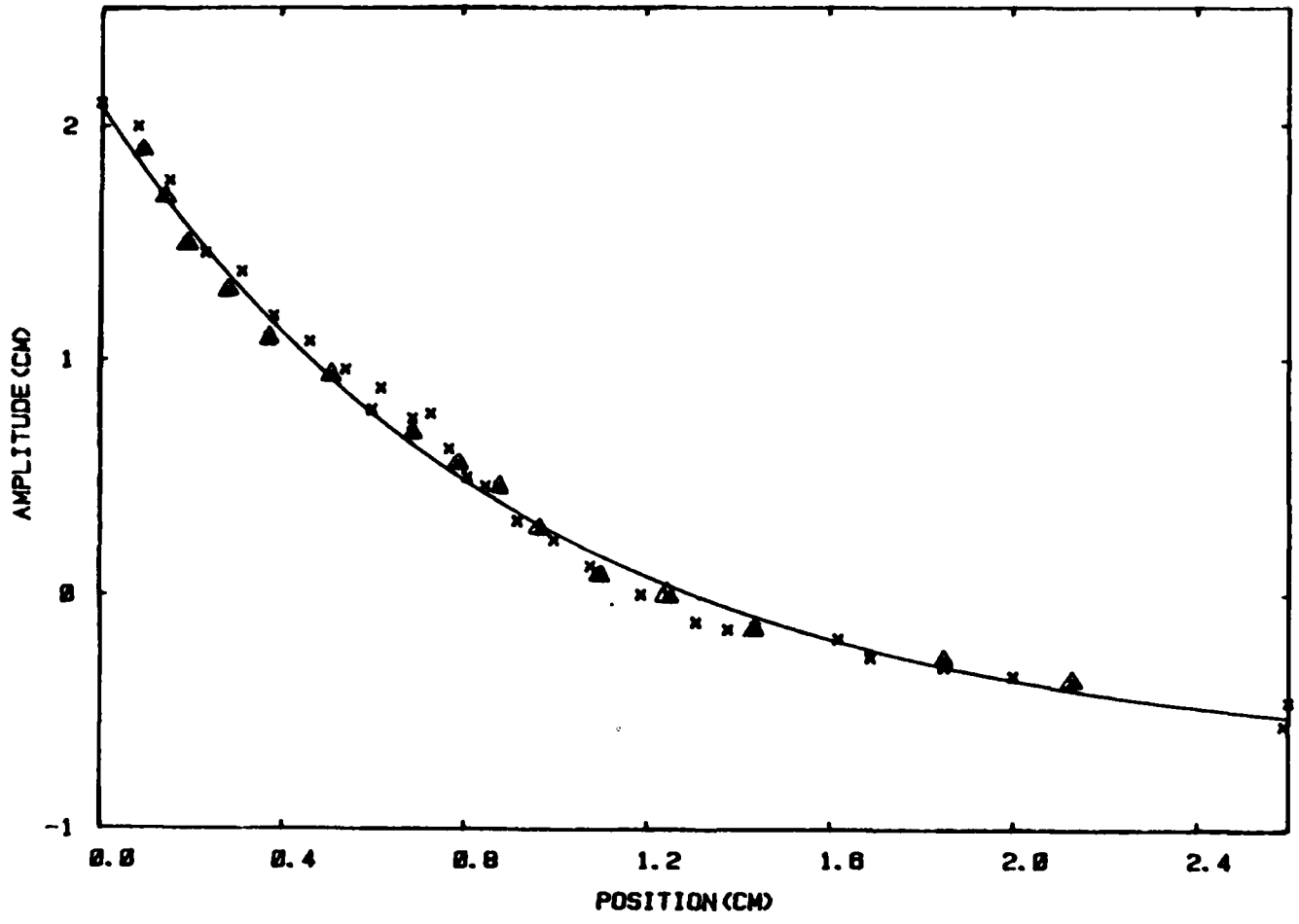

FIGURE 11. The profile of a soliton (f = 5.1 hz) as a function of y. The solid curve is $z = 2.8\exp(-1.1y) - 0.70$ cm. x and ▲ are experimental data taken from two pictures for the same soliton.

the higher the amplitude of the soliton. Outside the dashed boundary, changes in drive amplitude and/or frequency are generally hysteretic. If it exists, the soliton may be unstable, and there may be a mixture of modes. At a drive amplitude exceeding 0.081 cm, charateristically a competing mode rather than a soliton appears. As mentioned before, there is generally some degree of competition between the various modes of the trough, especially after the drive is just turned on. However, if the amplitude and frequency of the drive are appropriately set, energy will finally be sucked into a soliton and it becomes stable. Several ways are devised to selectively encourage the appearance of the soliton to the exclusion of competitive modes. One obvious way is to choose the trough dimensions which separate, in frequency, the unwanted modes from the soliton mode. Another way is to put sponge dampers at both ends of the trough so that the longitudinal modes are discouraged. Another very successful procedure is to nucleate the soliton mode by producing a local disturbance which is compatible with it. Thus sloshing motion across the width can be produced by rocking the resonator or with the help of a hand-held paddle. This can be very effective if it is done when the drive is just turned on. The self-focusing process described before is very striking if the soliton is generated by rocking the trough.

Since the frequency of the wave is half that of the drive, the phase of the drive is repeated every 180° of the wave.

Consequently solitons which are 0° or 180° apart in phase are compatible and equally driven. Thus the only steady state soliton pairs are in-phase solitons of the same polarity or 180° out-of-phase solitons of the opposite polarity. An opposite polarity soliton-pair can be generated by sharply twisting the trough about a central vertical axis, so that the sloshing in the left part has the opposite direction of that in the right part. Alternatively an inverted T-shaped paddle immersed in the water can be twisted to achieve the same result.

The interaction of the solitons was studied. Two solitons of the same polarity attract each other, but only weakly if the distance between them is significantly larger (say a factor of 3) than their characteristic length. Two solitons which start out 20 cm apart center to center, for example, take about 15 min to reach a separation where they strongly overlap. When this happen their attractive speed greatly increases. If the frequency is substantially lower than the small amplitude $\nu_{0,1}$, the two solitons combine; the end result is a single soliton having the amplitude of each of the initial ones. If the frequency is closer to $\nu_{0,1}$, the solitons oscillate through each other. Fig. 13 is a schematic of the stages of the oscillation. In the first stage, Fig.13(a), there is significant overlap. In Fig.13(b) the overlap is sufficient to create an amplitude at the center which is comparable with the amplitudes of solitons 1 and 2. In Fig.13(c) the solitons completely overlap. In Fig.13(d)

apparently solitons 1 and 2 have passed through each other and exchanged places while in Fig.13(e) the configuration is the original one. Left undisturbed this sequence repeats indefinitely. The longest period of time in which this phenomenon was observed is 36 hours. An interruption of the oscillation has never been seen except by accident or design.

A simple transducer which responds to wave heights is a pair of vertical wire electrodes that dip into the water. At a constant ac voltage drive, the current due to the conductance of the water is proportional to the wave height at the electrodes. Fig. 14 shows the response of such a transducer placed at the midpoint of the oscillating soliton-pair of Fig. 13. In the lowest trace, which covers the complete sequence of Fig.13, the paper speed was great enough so that the individual oscillations are seen (ν = 5.32 hz). The frequency of the envelope, which is much lower than the drive, is $2\nu/(156\pm0.5)$ = 0.068 hz. The upper traces are recorded at succesively slower paper speeds. Fig. 15 is the identical plot for the case that the fluid is pure alcohol. The principal difference is that the frequency of the oscillation is a little higher ($2\nu/(103\pm0.5)$ = 0.103 hz) than the water case. This suggests the surface tension might be playing an important role in the oscillation. The surface tension of alcohol is only one third that of water.

A pair of solitons of opposite polarity in close proximity

to each other repel each other and slowly move until they are approximately 12 cm apart, and then maintain this separation indefinitly. Again the interruption of this state has never been seen except by accident or design.

By introducing tracers (eccospheres) into the water we have been able to establish that the motion of solitons is one in which there is a transport of excitation with negligible transport of mass.

Essentially identical phenomena have been observed in an annular resonator 72 cm in mean circumference and 2.2 cm wide. This is interpreted to mean that the boundary conditions in the x-direction are irrelevant to our problem. As many as six solitons have been observed in the resonator. The polarity of solitons always alternates in the steady state limit.

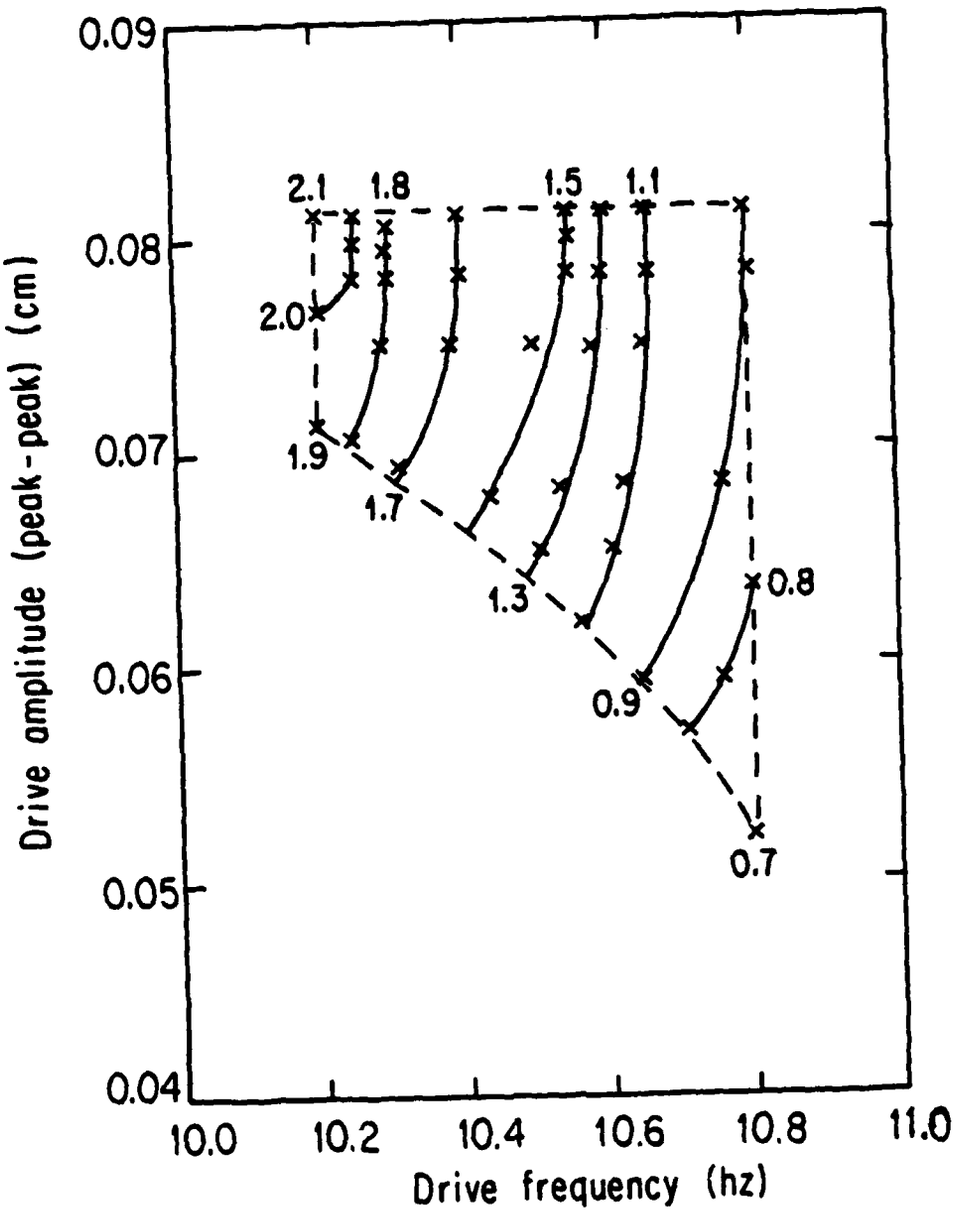

FIGURE 12. The range of drive amplitude and frequency in which individual solitons are observed without hysteresis.

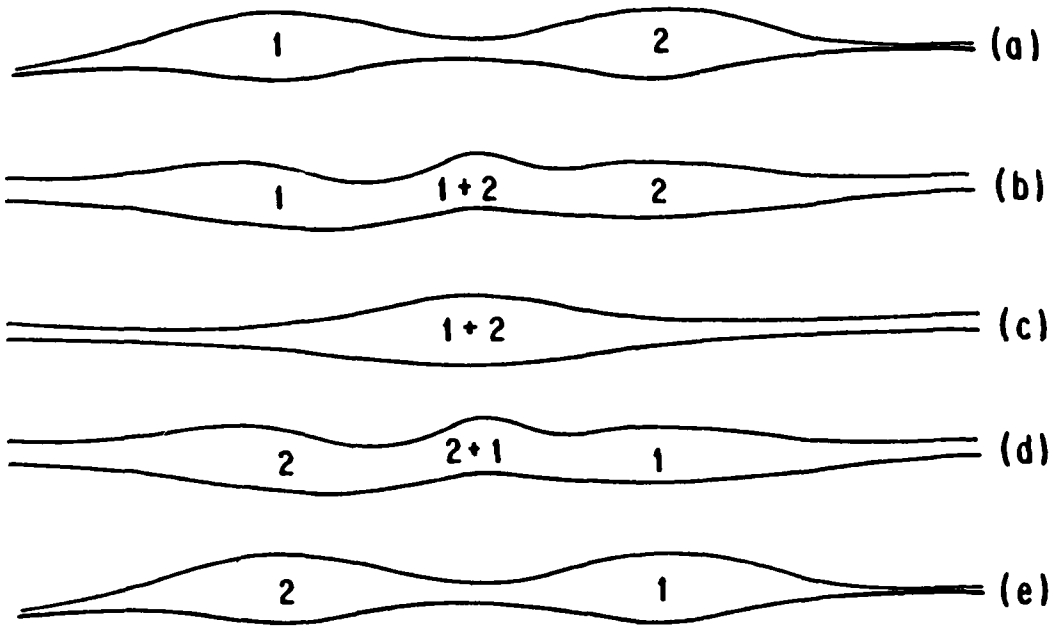

FIGURE 13. A schematic of stages in the resulting oscillation of two like-phase solitons.

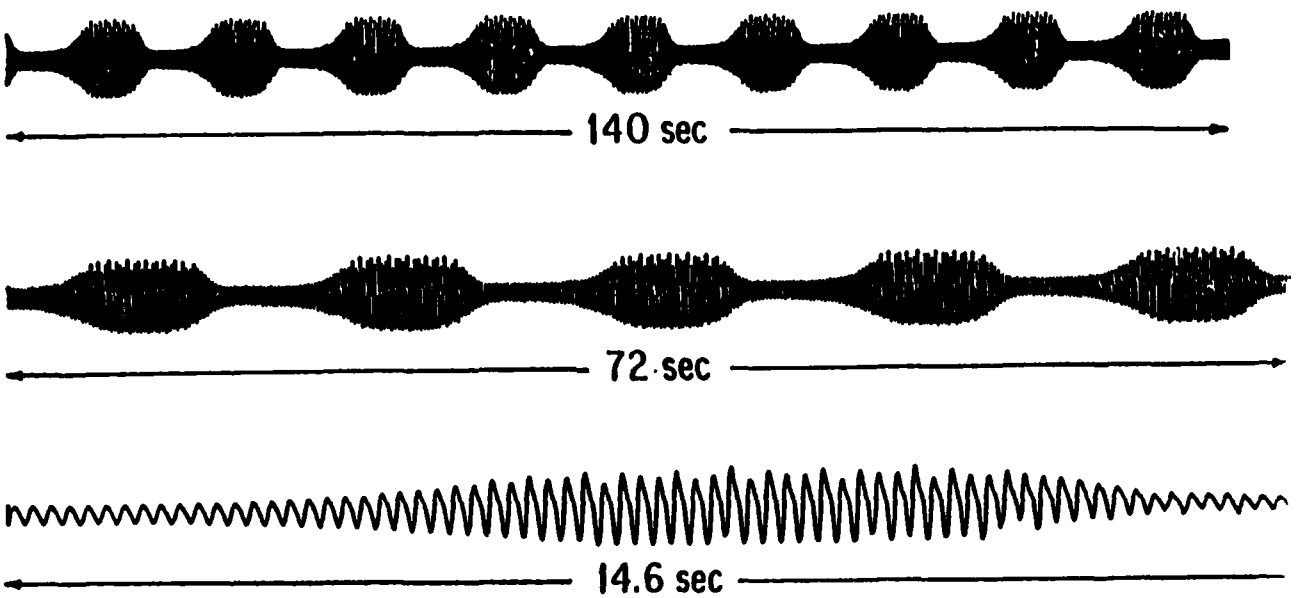

FIGURE 14 The response of a height transducer placed at the midpoit of the oscillating solitons of Fig. 13

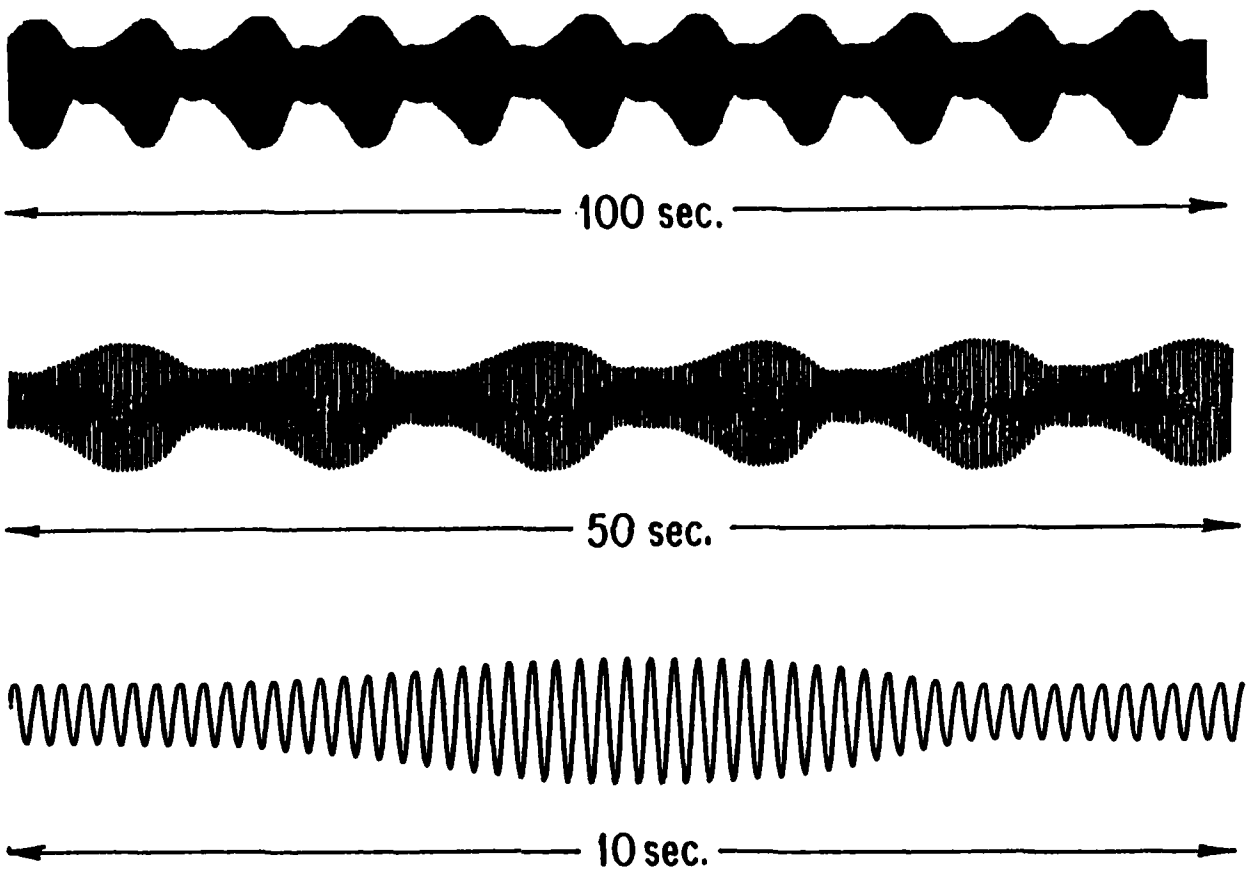

FIGURE 15. The identical plot of Fig. 14 for the case that the fluid filled in the trough is pure alcohol.

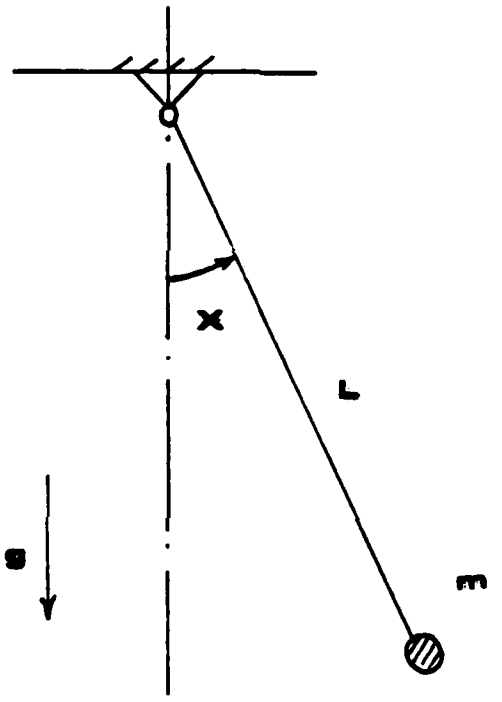

FIGURE 16 An undamped free oscillating pendulum.

CHAPTER III

A NONLINEAR PHYSICAL MODEL OF THE NONPROPAGATING SOLITON

'' The soliton digs its own hole
and builds its own walls.''
I. Rudnick

The experimental observations introduced in Chapter II can be summarized as follows.

(1) The system is very nonlinear as the amplitude of the soliton can be as high as water depth.

(2) The profile of the soliton in the x direction can be described by the hyperbolic secant function, which asymptotically approaches exponential decay function at its tails.

(3) The frequencies for getting the nonpropagating soliton is in a frequency range lower than the cutoff frequency given by Eq.(4). Moreover the higher the drive amplitude, the lower the optimal frequency for peak response.

(4) The nonpropagating soliton has the tendency to move to the shallow end where the cutoff frequency is lower.

What kind of the physical model can we use to describe the nonropagating soliton based on these experimental facts? A

reasonable model that would come up is that the cutoff frequency of the system becomes amplitude dependent as the system appears to be nonlinear. The fact that the drive frequency for getting the nonpropagating soliton is below the cutoff frequency suggests the model should be such that the higher the amplitude of the waves the lower the cutoff frequency. The simplest system which has this kind of property is an undamped free oscillating pendulum. When friction is neglected, the differential equation governing the motion of the pendulum is given by

$$\ddot{x} + \omega_0^2 \sin x = 0, \qquad (8)$$

where $\omega_0^2 = g/L$; the angle x designates the deviation from the vertical equilibrium position (Fig. 16). This is a nonlinear differential equation as we know the Taylor Series of sinx is given by

$$\sin x = x - x^3/3! + x^5/5! - x^7/7! + \ldots\ldots \qquad (9)$$

Only in the first order approximation, does Eq. (8) reduce to the linear differential equation:

$$\ddot{x} + \omega_0^2 x = 0, \tag{10}$$

Then the resonant frequency of the system is independent of the angle. For large angles the linear approximation is not justified. If the second term of the expansion is also included, Eq. (9) becomes

$$\ddot{x} + \omega_0^2 x - (\omega_0^2/6)x^3 = 0. \tag{11}$$

This is the Duffing equation[15]. The solution (up to third order) of the nonlinear differential equation can be written as

$$x = a\sin(\omega t + \gamma) + \omega_0^2/(192\omega^2)a^3\sin(3\omega t + 3\gamma), \tag{12}$$

where ω is amplitude dependent and is given by the following equation:

$$\omega^2(a) = \omega_0^2 - (\omega_0^2/8)a^2. \tag{13}$$

Now let us use this model to understand the self-trapping effects of the nonpropagating soliton. At the core of the

soliton the peak amplitude at the wall is so high that the corresponding cutoff frequency there is significantly lower than the small amplitude cutoff frequency given by Eq. (4) according to our model. However the linear theory is still valid at both wings of the nonpropagating soliton since the amplitudes there are pretty small. If the system is driven at the frequency higher than the amplitude dependent cutoff frequency at the core and lower than the small amplitude frequency at the wings, the energy, which propagates out of the core, gets totally reflected at the wings, and the wave becomes evanescent. This self-trapping is reminiscent of polaron behavior in crystals, and leads to the soliton being called a hydrodynamic polaron.

Consider Fig. 7. The soliton profile in the x direction is described by z = 2.1sech(x/1.12)cm. At the core the peak amplitude at the wall is 2.1 cm , consequently the cutoff frequency is lower than that at the wings. At the tails of the hyperbolic secant function the decay length, 1.12 cm, is equal to the low amplitude waveguide evanescent length, and this is just the magnitude of $1/k_x$. Thus we can determine the phase velocity, c, by the following equation:

$$c = \omega/(k_x^2 + k_y^2)^{\frac{1}{2}}$$
$$= 2\pi x 5.1/[(\pi/2.6)^2 - (1/1.12)^2]^{\frac{1}{2}}$$
$$= 37.7 \text{ cm/sec.}$$

Eq. (1) gives the value 33.7 cm/sec. This simple calculation shows that our model is reasonably good.

By using this model it is not difficult to understand the self-focusing effects observed at the initial stage of the process of the soliton formation. As the drive amplitude passes the threshould value of the parametric instability, the amplitude of the excitation starts to develope. Wherever the amplitude is higher, the amplitude dependent cutoff frequency becomes lower. As has already been pointed out that the energy of the excitation likes to go to the place where the cutoff frequency is lower. In a snowball-like process, the energy builds up in a very small region, and the soliton is formed. Once the soliton appears it is stable due to the above-mentioned self-trapping mechanism. Another fact which is important to the stability of the soliton is the dispersion of the system. If there is no dispersion, shock waves form and there is abundant energy dissipation.

CHAPTER IV

MEASUREMENTS OF TUNING CURVES

As pointed out earlier the necessary conditions for creating a nonpropagating soliton is that a nonlinear dispersive system has an amplitude dependent cutoff frequency such that the higher the amplitude the lower the cutoff frequency. Therefore in order to test our physical model it is necessary to measure the amplitude dependent resonant frequency of (0,1) mode of our trough.

A. INTRODUCTION

The amplitude dependent resonant frequency of (0,1) mode calculated by J. Miles[2], and by A. Larraza and S. Putterman[3] is given by the following equation (Eq. (E-24), Appendix E):

$$\nu_e(\zeta) = \nu_e[1-Ag^2\zeta^2/(128W^4\zeta^4)] \qquad (14)$$

where ν_e is determined by Eq. (4), and A is given by Eq.(E-20)

(Appendix-E) as

$$A = \frac{1}{8}\left(6T^4 - 5T^2 + 16 - T^{-2} \right) \qquad (15)$$

where $T = \tanh(\frac{\pi}{W}d)$. When correction is made for surface tension Eq. (E-20) becomes Eq. (E-22) as

$$A = \frac{1}{2}[1+(1-T^2)^2+\frac{1}{2}(1+4\mu^*)^{-1}(1+T^2)^2 -\frac{1}{4}(T^2-4\mu^*)^{-1}(3-T^2)^2] \qquad (16)$$

where μ is surface tension, and $\mu^* = \mu(\frac{\pi}{W})^2/(\rho g)$. From Eq. (14) it is obvious that the amplitude dependent frequency ν can be greater or less than ν_0 depending on the sign of A, which is in turn uniquely determined by the depth of the liquid. By putting A = 0 in the equation the theoretical crossover depth can be calculated. Experimentally $\nu_0(\zeta)$ can be determined by measuring the tuning curve of the (0,1) mode for various amplitudes, ζ, of the surface-wave oscillation for different depths of liquid. By using the measured value of ν_0 - the peak response frequency at small amplitude, $\nu_0(\zeta)$ - the peak response frequency at high amplitude , ζ, when we sweep the frequency for different drive amplitudes, the magnitude as well as the sign of the nonlinear coefficient, A, can be determined from the Eq. (14).

B. APPARATUS

The resonator used to measure the tuning curve is a sealed glass basin with the inside dimensions of L 2.0 × W 2.6 × H 7.0 in centimeters.

The reason for not using the long channel (38 cm) to determine the tuning curve is that when the amplitude of the surface-wave gets quite high, solitons appear in the long channel. The 2cm length is chosen to be smaller than the characteristic length of the soliton so that the soliton does not appear and so that the fundamental resonant frequency of the longitudinal (1,0) mode is well above that of the (0,1) mode. Then the tuning curve is that of the transverse (0.1) mode, and as pointed out earlier, this is the equivalent of being at the first cutoff frequency for a waveguide of infinite length.

The resonator is cleaned with a potassium hydroxide, ethyl alcohol, solution followed by washing with hot tap water and ethyl alcohol. Then it is filled with 100% ethyl alcohol up to the depth of d as the working fluid. The resonator is put on an improvised table on rollers which is driven horizontally by a 5 inches loudspeaker in a direction normal to the sides of the basin so that sloshing occurs across the width of the basin (Fig. 15). An accelerometer (4367, Bruel Kjaer) is used to measure the displacement of the oscillating table. It is found that the displacement is quite sinusoidal -- the second harmonic component is at least 40 db lower than the fundamental.

C. ELECTRONICS

The block diagram of the eletronics is shown in Fig. 16. The oscillator (Wavetek) is slowly swept over the range of 3 - 7 hz by using an external ramp voltage signal. The output of the oscillator drives the loudspeaker after going through a power amplifier. In order to keep the displacement amplitude of the oscillating table constant when the frequency is changed, a feedback loop is used. The basic principle is as follows. An ac voltage signal from the accelerometer proportional to the oscillating table displacement is sent to the charg amplifier (2635, Bruel & Kjaer) then is rectified and filtered by an ac - dc converter. A dc differential amplifier is used, its negative input is connected to the output of the ac - dc converter and its positive input is controlled by a dc regulated power suply. Thus the amplified negative dc signal from the output of the dc differential amplifier is related to the displacement amplitude of the oscillating table in such a way that the higher the displacement amplitude the more negative the dc output. This negative dc voltage is sent to the VCA input of the Wavetek to decrease the amplitude of the ac output of Wavetek. The result of this simple feedback loop is quite good; it makes the driving system which originally has a peak in response at about 5 hz to become a constant amplitude of displacement driving source.

The transducer for measuring the displacement of the surface-wave is a pair of vertical wire electrodes that is immersed into the liquid. A built-in low output impedance (600Ω) ac voltage (1 v, 1000 hz) from lock-in amplifier (HR - 8, Princeton Applied Search) is applied on the transducer, which is in series with a 100Ω resister. Since the resistance of the resister is negligible comparing with the impedance of the liquid between the electrodes (about 100 kΩ), the voltage drop across the resister is proportional to the conductance of the liquid between the pair of electrodes. When the height of liquid oscillates at about 5 hz as the surface-wave does, the ac conductance of the liquid at the transducer is modulated. The lock-in amplifier picks up the slow modulation signal, amplifies it and sends it to the ac - dc converter. An x-y recorder is used to plot out the tuning curves.

D. THE RESULTS OF MEASUREMENTS

Typical frequency sweeps for several different drive amplitudes for each of six different depths, d, are shown in Figs. 19 - 25. It is evident as shown in Fig. 19 that when d = 0.5 cm the peak frequency increases as the amplitude of water-surface-wave becomes bigger. ν_e is 4.22 hz from Eq.(4) in good agreement with the observed 4.23 hz. As the amplitude, ζ, goes from 0.1 cm to 0.4 cm in steps of 0.1 cm, the peak

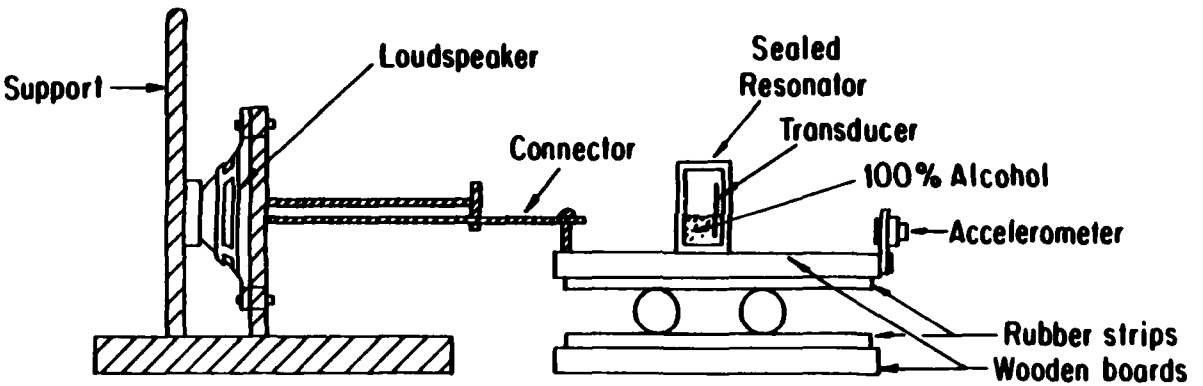

FIGURE 17 Schematic of the apparatus with direct drive.

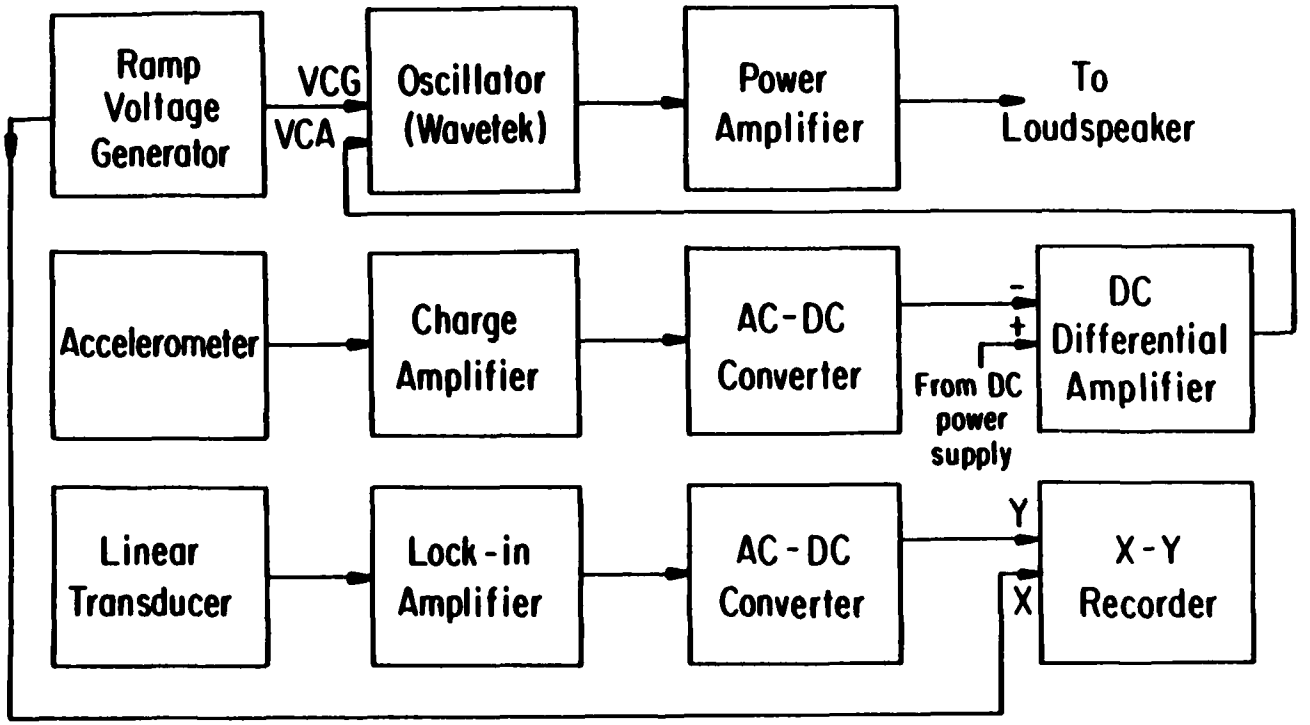

FIGURE 18 The block diagram of the electronics.

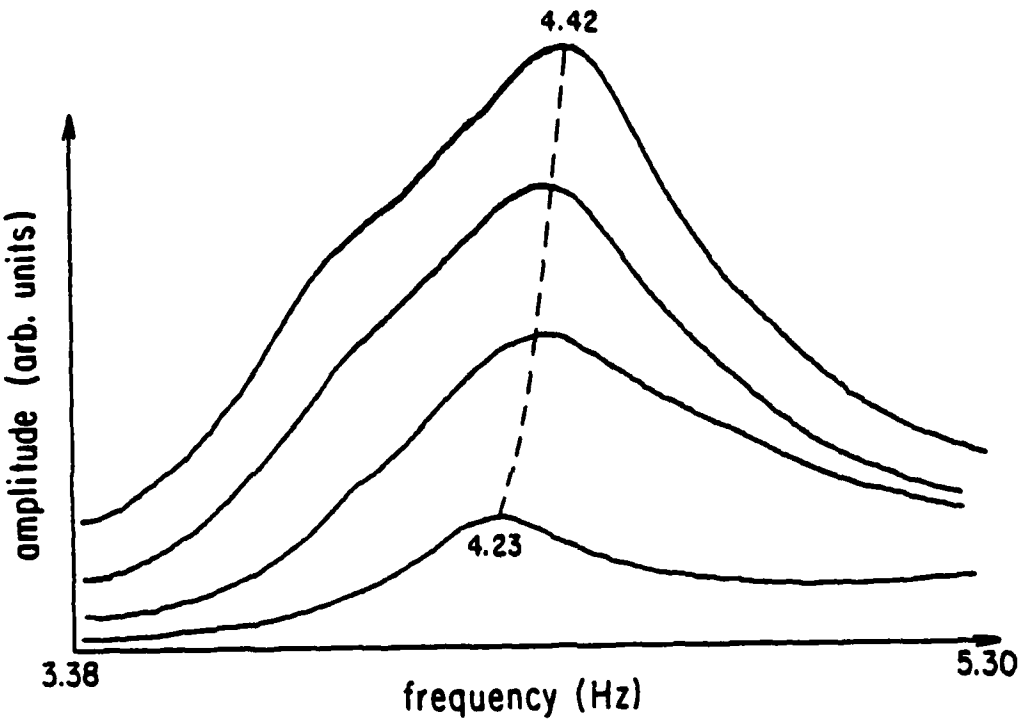

FIGURE 19 The (0,1) mode amplitude dependent tuning curves of a rectangular section resonator (W = 2.6 cm), d = 0.5 cm.

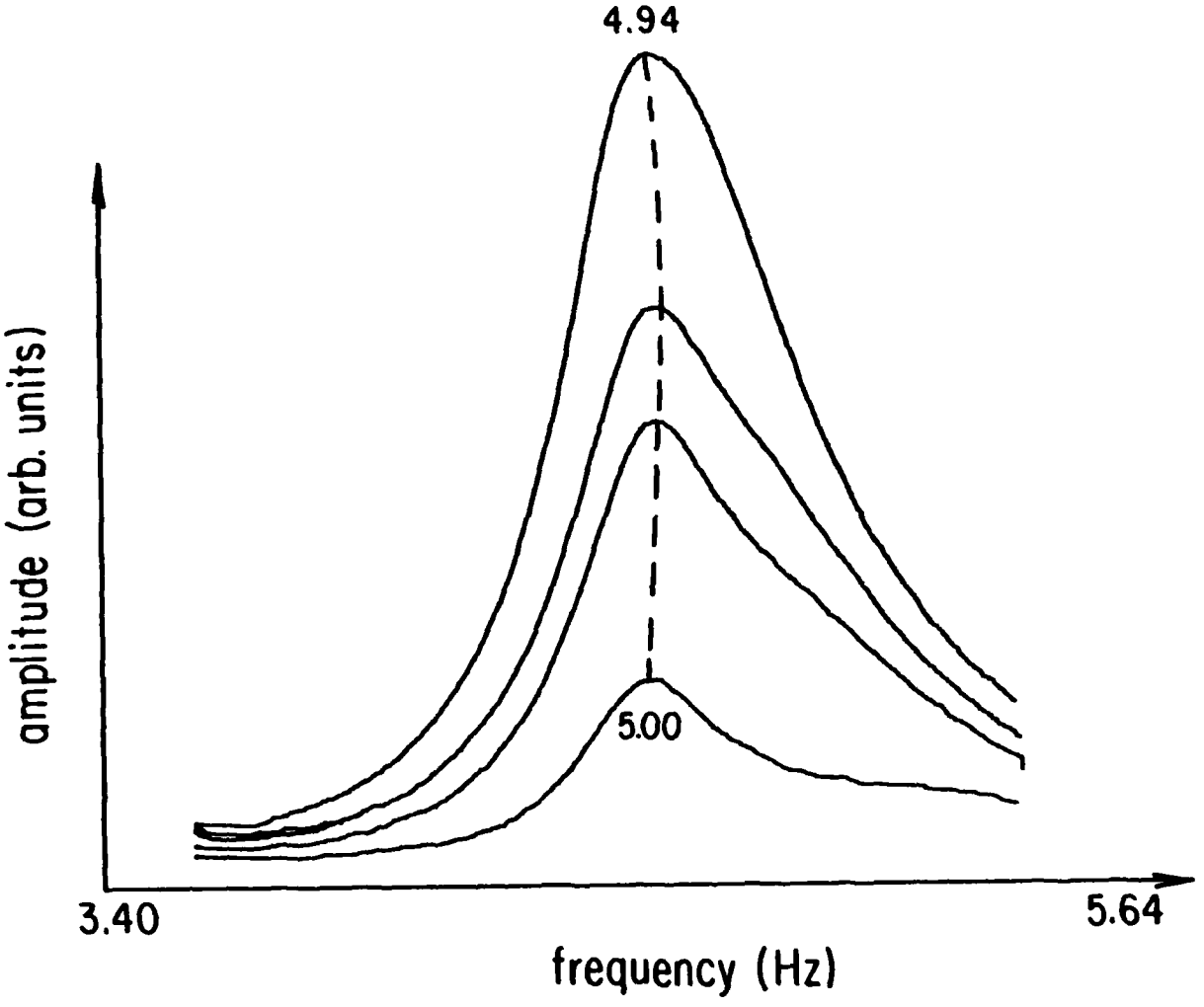

FIGURE 20. The (0,1) mode amplitude dependent tuning curve of the same resonator, d = 1.0 cm.

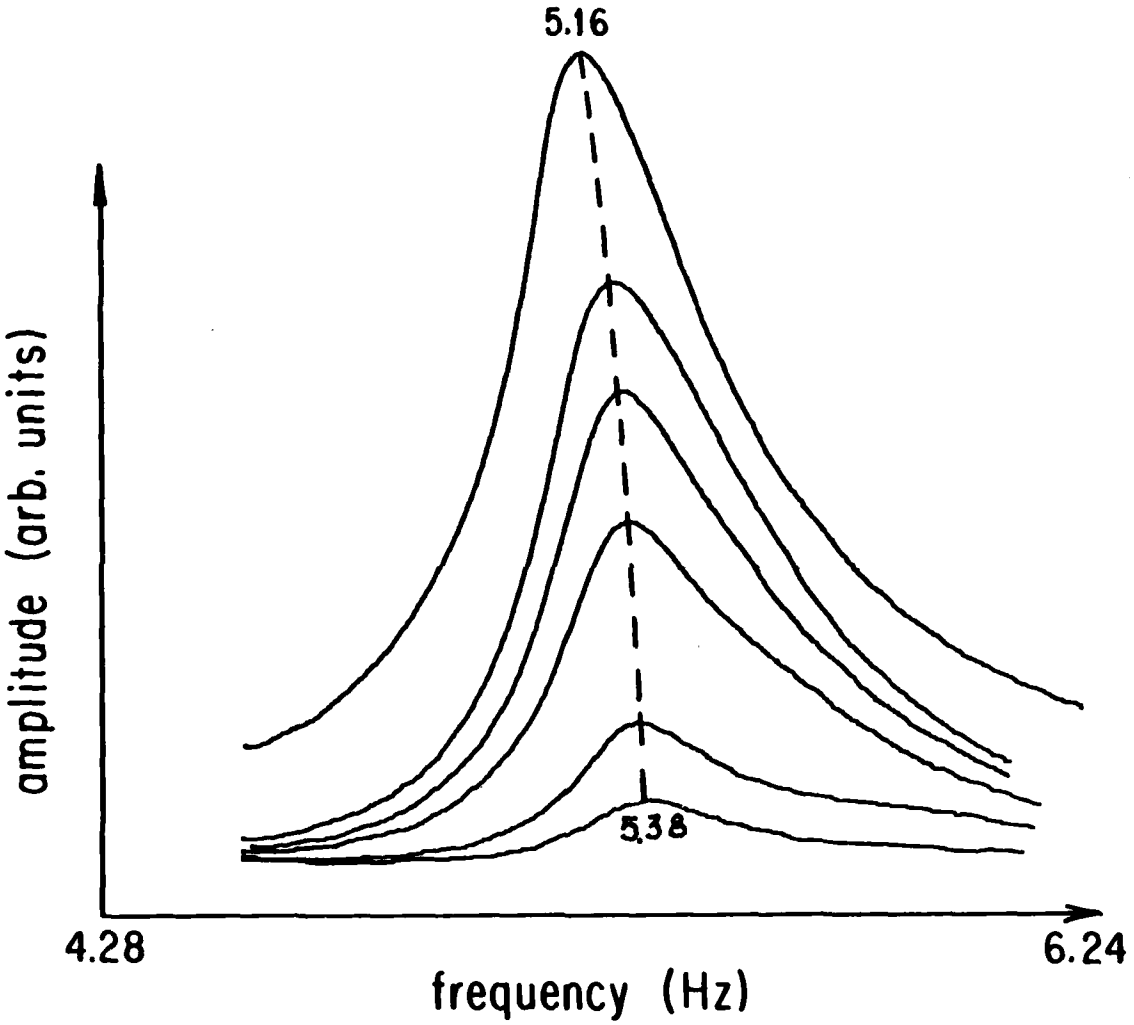

FIGURE 21. The (0,1) mode amplitude dependent tuning curves of the same resonator, d = 1.5 cm.

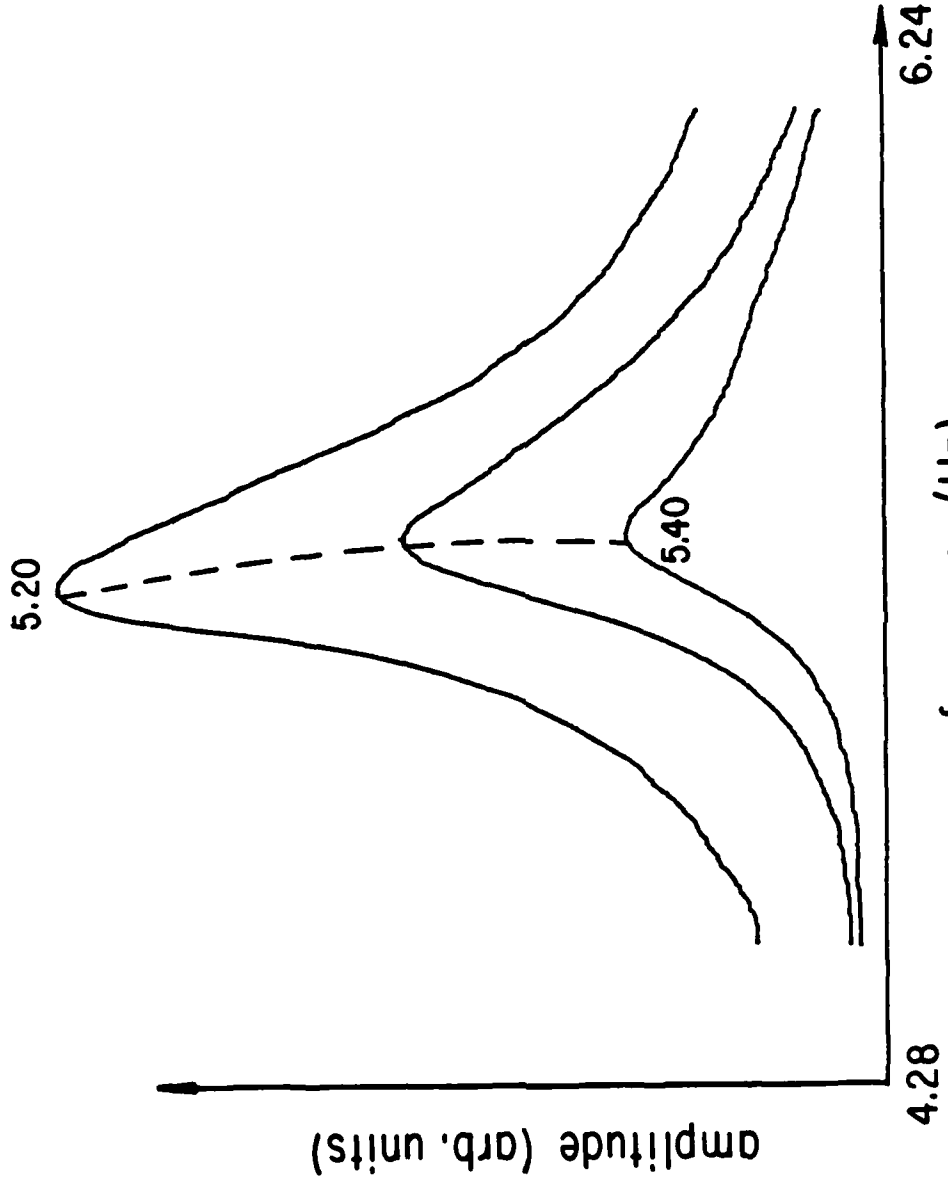

FIGURE 22. The (0,1) mode amplitude dependent tuning curves of the same resonator, d = 1.7 cm.

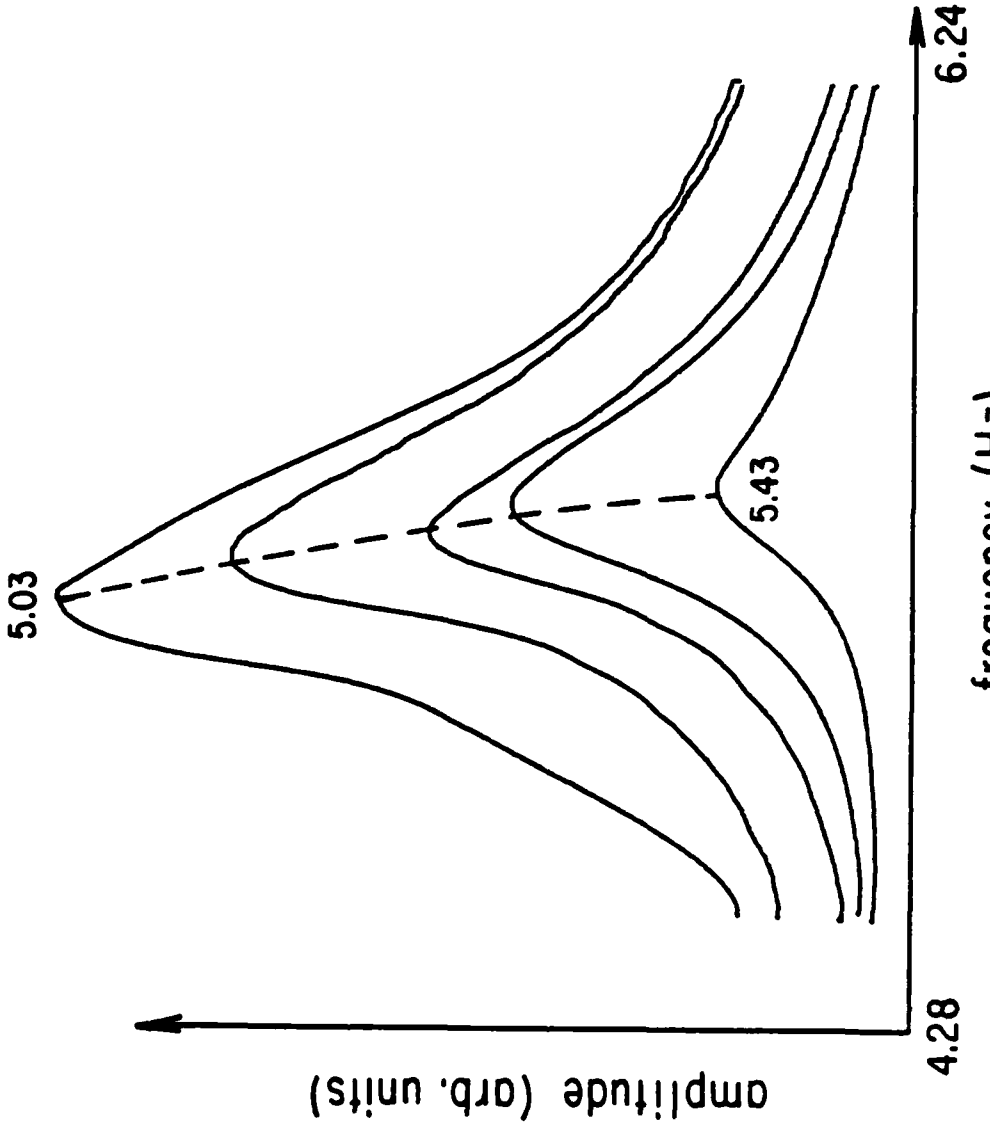

FIGURE 23. The (0,1) mode amplitude dependent tuning curves of the same resonator, d = 2.0 cm.

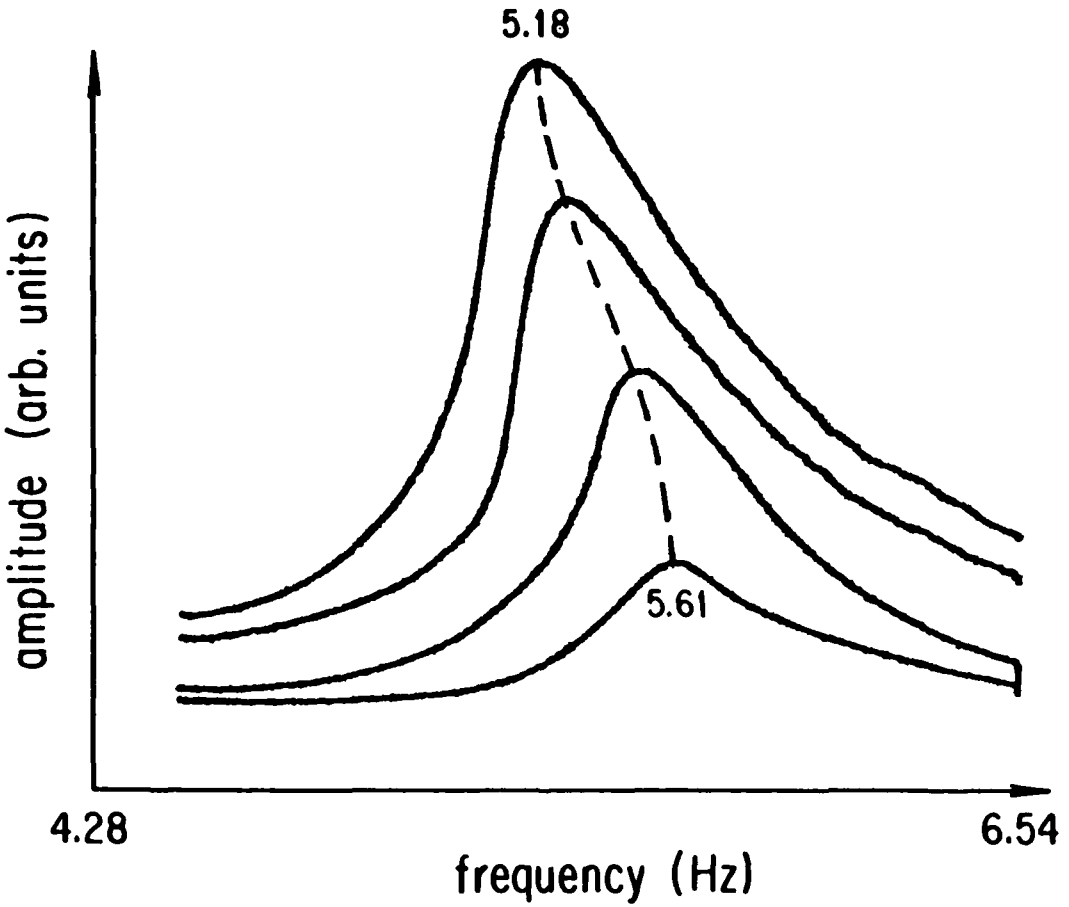

FIGURE 24. The (0,1) mode amplitude dependent tuning curves of the same resonator, d = 3.0 cm.

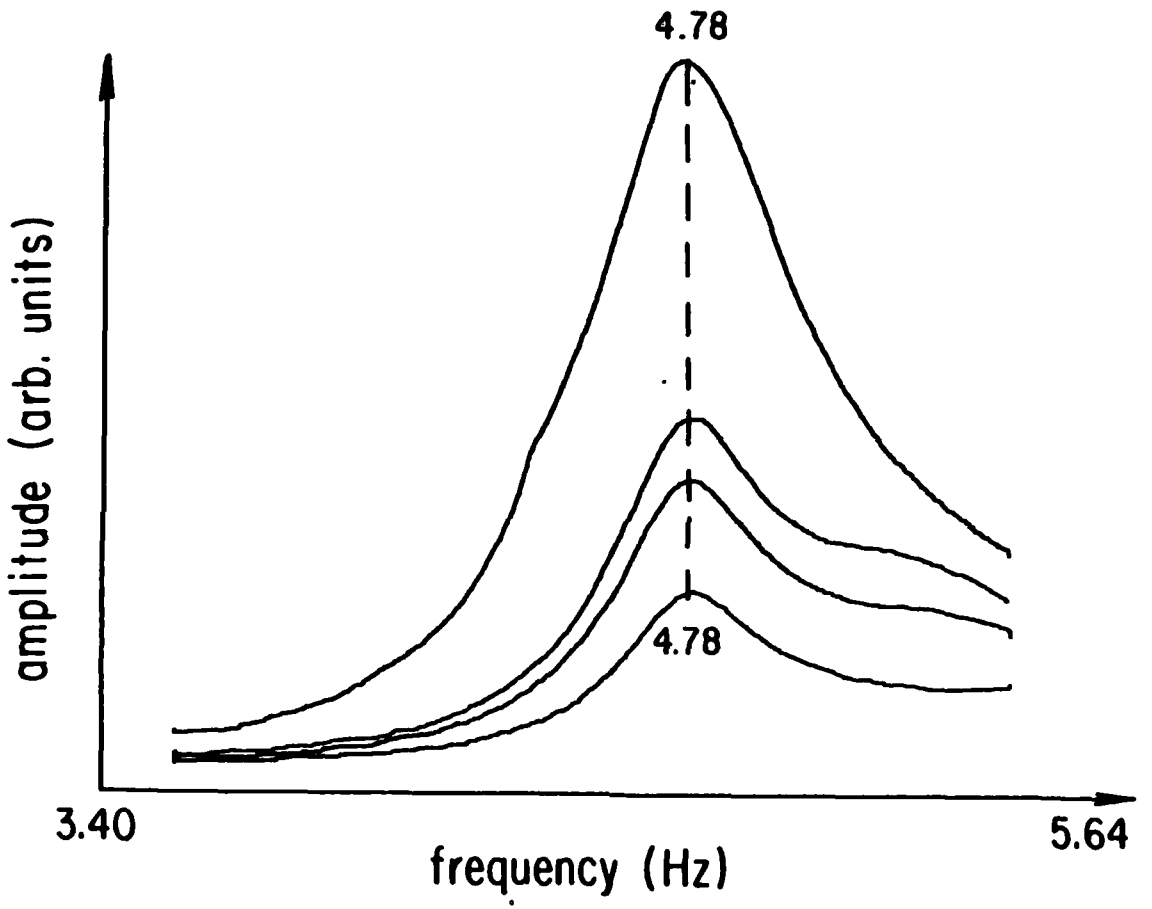

FIGURE 25. The (0,1) mode amplitude dependent tuning curves of the same resonant, d = 0.8 cm.

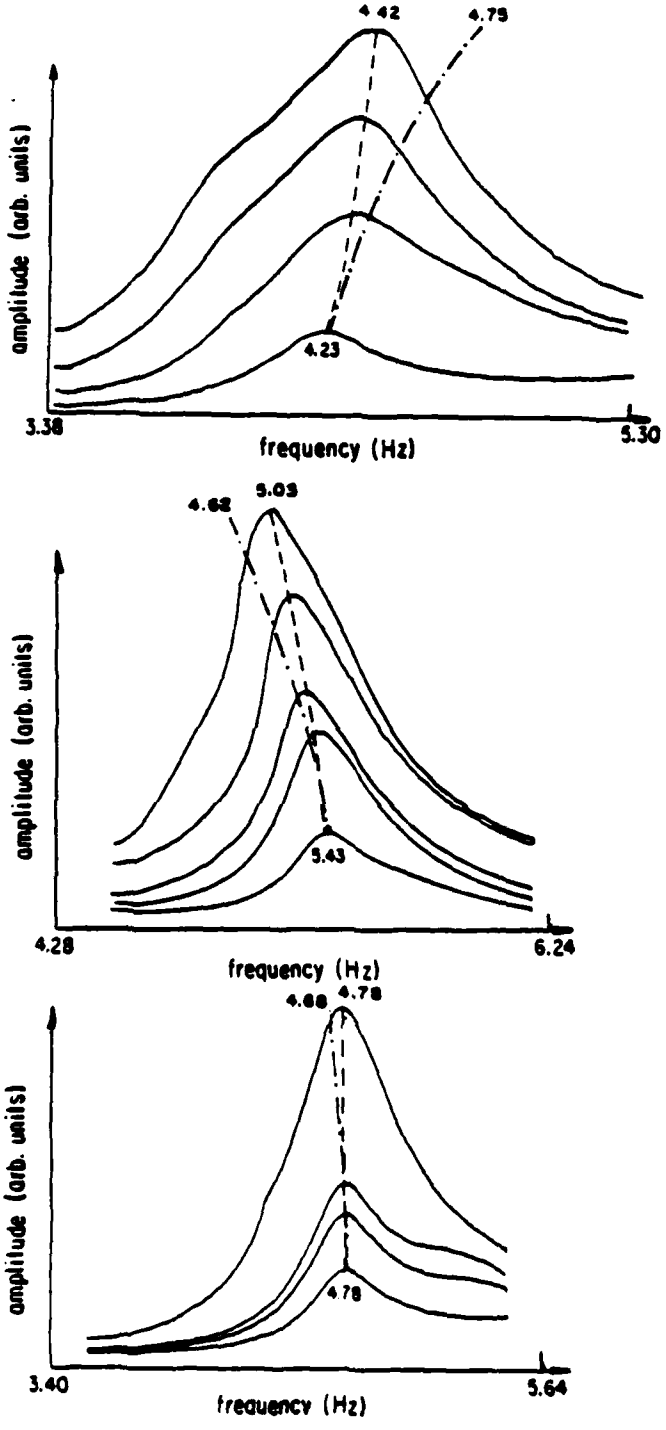

FIGURE 26. A reduced plot of the combination of Figs. 19, 23, and 25 for comparison with the theory.

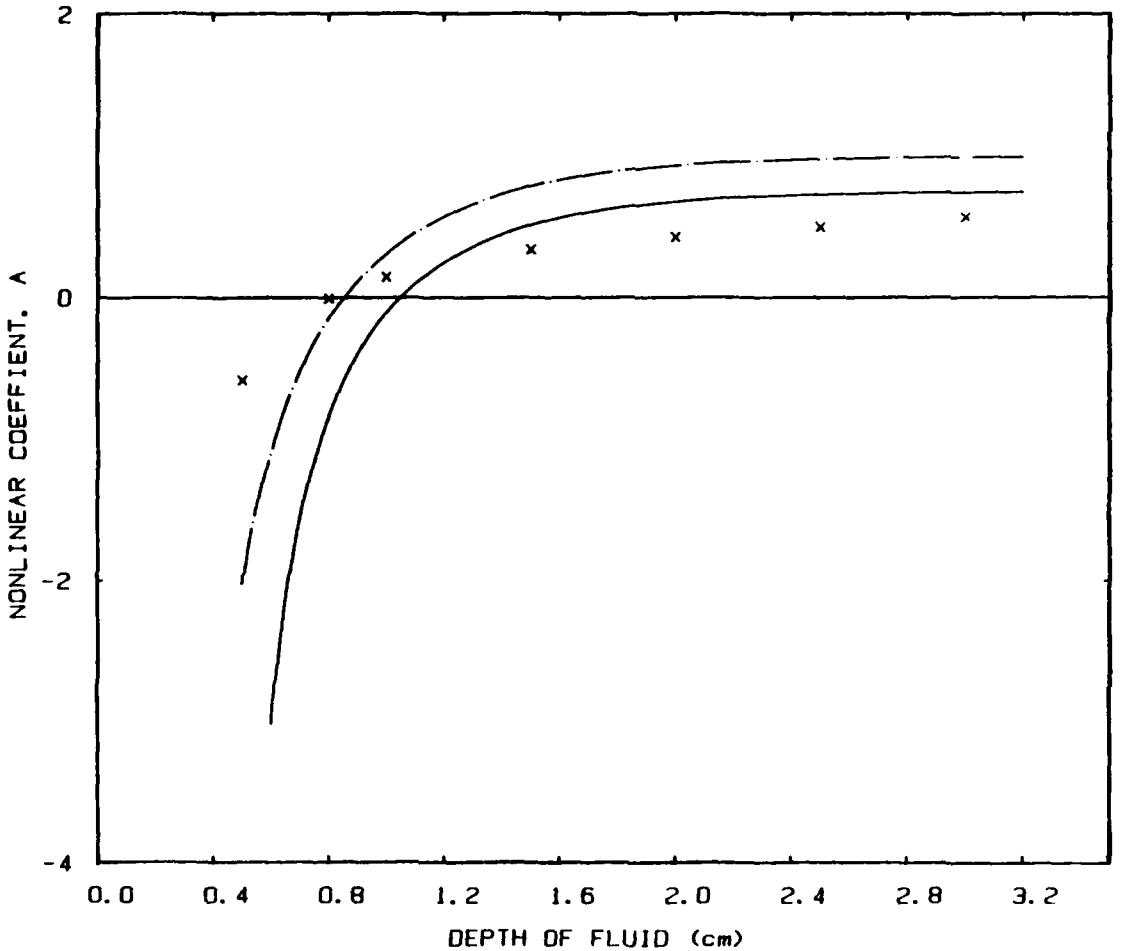

FIGURE 27. A plot of the nonlinear coefficient, A, versus fluid depth d.

frequency shifts up from 4.23 hz to 4.42 hz. This is a typical right bending tuning curve.

Figs. 20 - 24 are respectively for the case of d = 1.0, 1.5, 1.7, 2.0, and 3.0 cm. The common feature is that the peak frequencies all shift down as the amplitudes of the responses go higher and higher; all belong to left bending tuning curves. Fig. 20 (d = 1.0 cm) shows that the peak frequency goes from 5.00 hz down to 4.94 hz as the amplitude goes from 0.2 cm up to 0.8 cm. Fig. 21 (d = 1.5 cm) shows that the peak frequency goes from 5.38 hz down to 5.16 hz as the amplitude goes from 0.1 cm up to 0.7 cm. Fig. 22 (d = 1.7 cm) shows that the peak frequency goes from 5.4 hz down to 5.20 hz as the amplitude goes from 0.2 cm up to 1.0 cm. Fig. 23 (d = 2.0 cm) shows that the peak frequency goes from 5.43 hz down to 5.03 hz as the amplitude goes from 0.2 cm up to 1.0 cm in steps of 0.2 cm. Fig. 24 shows that the peak frequency goes from 5.61 hz down to 5.18 hz as the amplitude goes from 0.2 cm up to 0.9 cm.

Fig 25 is a plot for the case of d = 0.8 cm. Within the experimental error the peak frequency remains constant at 4.78 hz, as the amplitude of the wave increases from 0.1 cm to 0.8 cm. It was experimentally found that at d = 0.8 cm changes in depth of 0.1 cm produced hardly detectable shifts of peak frequency. It is concluded that it is at this depth (d = 0.8 ± 0.1 cm) that the crossover from right leaning to left leaning occurs. The

calculated value of ν_0 is 4.81 hz from Eq. (4).

Figure 26 is a reduced plot of the combination of Figs. 19, 23, and 25. The dash dot curves are theoretical peak values from Eq. (E-24).

Fig. 27 contains plots of the nonlinear coefficient, A, versus fluid depth, d. The top curve is for the case without surface tension correction i.e. Eq. (15) and the bottom curve is for the case with a surface tension correction i.e. Eq. (16). As shown by Eq. (14) the nonlinear coefficient, A, for various depths of liquid can be calculated when the measured values of ν_0, $\nu_0(\zeta)$ and ζ are plugged into the Eq. (E-22). Thus the experimental value of A can obtained from the data of Figs. 19 - 25, and represented by the points on Fig. 27. From the curves we can get an independent determination of the crossover depth to compare with the above-mentioned experimental value (0.8 cm). This is the value of d at which A vanishes. The intersection of a horizontal line, A = 0, with the top curve yields a value of d = 0.85 cm and for the bottom curve, d = 1.03 cm.

From Figs. 26 and 27, we can see that the curve for Eq.(16) is closer to the experimental data than the curve for Eq.(15) at deep-water region. The reverse is true for the crossover depth. Overall both equations work better in the deep-water region than shallow-water region. The reason for this is, as pointed by A.

Larraza, a result of a breakdown of the pertubation theory as the system approaches the nondispersive limit at zero depth.

In summary, experimental measurements shows that a rectangular section resonator (W = 2.6 cm) has an amplitude dependent tuning curves with a peak frequency, ν_p, such that

$$d\nu_p/d\zeta < 0, \text{ for } d > 0.8 \text{ cm},$$
$$d\nu_p/d\zeta = 0, \text{ for } d = 0.8 \text{ cm},$$
$$d\nu_p/d\zeta > 0, \text{ for } d < 0.8 \text{ cm}.$$

The nonlinear coefficient, A, as a function of depth, d, is found to be in reasonable agreement with the theoretical results of Miles[2], and Larraza and Putterman[3]. As to the discrepancy between theory and experiment, especially at the high amplitude limit, Professor Putterman expressed his satisfaction with the extent of agreement. He often emphasizes the theory is a perturbation calculation good only to third order in $\frac{\pi}{W}\zeta << 1$, which is much smaller than the amplitudes used in the experiment.

CHAPTER V

THE FREE DECAY RATE OF THE NONPROPAGATING SOLITON

A. WATER-SURFACE-WAVE DAMPING IN CLOSED BASINS

The damping of water-surface-wave in a closed basin has been extensively studied by Benjamin[16], Ursell[17], Case, Parkinson[18], Keulegan[19], Van Dorn[20] and Miles[21]. If we use δ_w and δ_s to respectively represent the decay rate due to the viscous disippation in the neighborhood of the rigid wall and in the neighborhood of the free surface, and δ_L to denote the decay rate due to the capillary hysteresis associated with the meniscus formed at the contact line between the free surface and the rigid wall, in general δ_L will be much smaller than the other two for our case. It was shown theoretically by Ursell[16], Case and Parkinson[18] that for a clean bounded surface δ_s is negligible comparing with δ_w. While experimental measured value of δ/δ_w may be as large as three. Van Dorn[19] clarified the discrepancy by his experiment, he found that the decay rate agreed with δ_w when the water was fresh, then the former tended to increase with time to some higher limiting value within an hour or so. He attributed the observed higher value of δ_s to a surface film produced by spontaneous contamination. Considering these effects

Miles[21] derived the following equations:

$$\delta_w = \frac{W}{2\pi}k\left(\frac{2\eta}{\rho\omega}\right)^{\frac{1}{2}}\left(1+\frac{W}{L}+\pi\left[1-\left(\frac{2d}{W}\right)\right]\operatorname{cosech}\left(\frac{2\pi d}{W}\right)\right) \qquad (17)$$

$$\delta_s = \frac{\omega}{4}k\left(\frac{2\eta}{\rho\omega}\right)^{\frac{1}{2}}\left(C_r-C_i\right)\coth\left(\frac{\pi d}{W}\right) \qquad (18)$$

$$\delta_L = \frac{32\kappa}{\pi}\left(1+\frac{\pi L}{2W}\right)\left[\mu/(\rho g L\zeta)\right] \qquad (19)$$

where μ is the surface tension, L is the length of the basin, η is the viscosity, (C_r-C_i) the ratio of the surface-film damping to that which would be produced by an inextensible film, may be approximately taken between 0 and 1 for low frequency water-surface-wave depending the extent of contamination at the surface, κ is a semiemperical coefficient which is related to capillary hysteresis at the meniscus on the wall, it may be approximated by 0.05 for a hydrophilic basin (e.g. clean water on glass).

B. FREE DECAY MEASUREMENTS

A sealed glass channel, filled with 100% ethyl alcohol up to 2 cm, with the inside dimensions of L 38× W 2.6× H 7.0 in centimeters is used to measure the free decay rates of the low amplitude oscillation of the (0,1) mode as well as the solitons.

Let us first to calculate the decay rate of the (0,1) mode by using the above-mentioned formula worked out by Miles. Substituting the following data into the Eqs. (17) to (19):

$L = 38cm$, $W = 2.6cm$, $d = 2.0cm$

$\mu = 23$ dyne/cm, $\rho = 0.79$ g/cm^3, $\eta = 0.012$ g/(sec•cm)

$\kappa = 0.05$, $\omega = 2\pi \times 5.1$ rad/sec, $0 < (C_r - C_i) < 1$

we get

$$\delta_w = 0.2 \text{ sec}^{-1}$$

$$0 < \delta_s < 0.3 \text{ sec}^{-1}.$$

$$\delta_L = 0.02 \text{ sec}^{-1}.$$

Thus $0.2 \text{ sec}^{-1} < \delta < 0.5 \text{ sec}^{-1}$.

Since we known from experiments that the main dissipation comes from the walls and the surface of the liquid, the channel is carefully cleaned by using the same procedure as the one we used to clean the small basin before the tuning curves were

measured. Right after being filled with 100% ethyle alcohol as the working fluid, the channel is sealed, thus the contamination at the liquid surface would be minimized.

Fig. 28 is the plot of a decaying (0,1) mode surface-wave with the frequency of 5.1 hz and the initial amplitude of 0.5 cm. Decay rate is determined to be 0.4 sec^{-1}, which is in the range of the theoretical prediction.

The free decay rate of the soliton was determined in two different ways. In one the channel is driven by the oscillating table in its width direction, and once the soliton is created and reaches a stable state, the driving source is turned off. The free decaying oscillation data were stored in a wave analyser (6000, Data Precision) and plotted out by a x-y recorder. In the other method the channel is oscillated vertically at twice the soliton frequency by a vibration exciter (4809, Brue14Kjaer). Identical decay rates were obtained for both methods.

Fig. 29 is a plot of the free decay soliton with the initial peak amplitude of 1.8 cm and the frequency of 5.1 hz. Comparing with Fig. 28 clearly the soliton decays faster than the corresponding (0,1) mode initially. Fig. 30 is a plot of the amplitude versus time. The points are the amplitudes of the same soliton as Fig. 29, and the circles are the amplitudes of the same (0,1) mode surface-wave as Fig. 28. From the plot we can see the initial decay rate of the soliton (frequency = 5.1

hz, amplitude = 1.8 cm) is 0.7 sec^{-1} and changes to 0.4 sec^{-1} as its amplitude drops below 0.5 cm, which is seen to be the same as the decay rate of the corresponding small amplitude transverse mode. The possible expanation of the higher initial decay rate is that the soliton has very rich higher harmonic components which in general decay faster than the fundamental of the (0,1) mode.

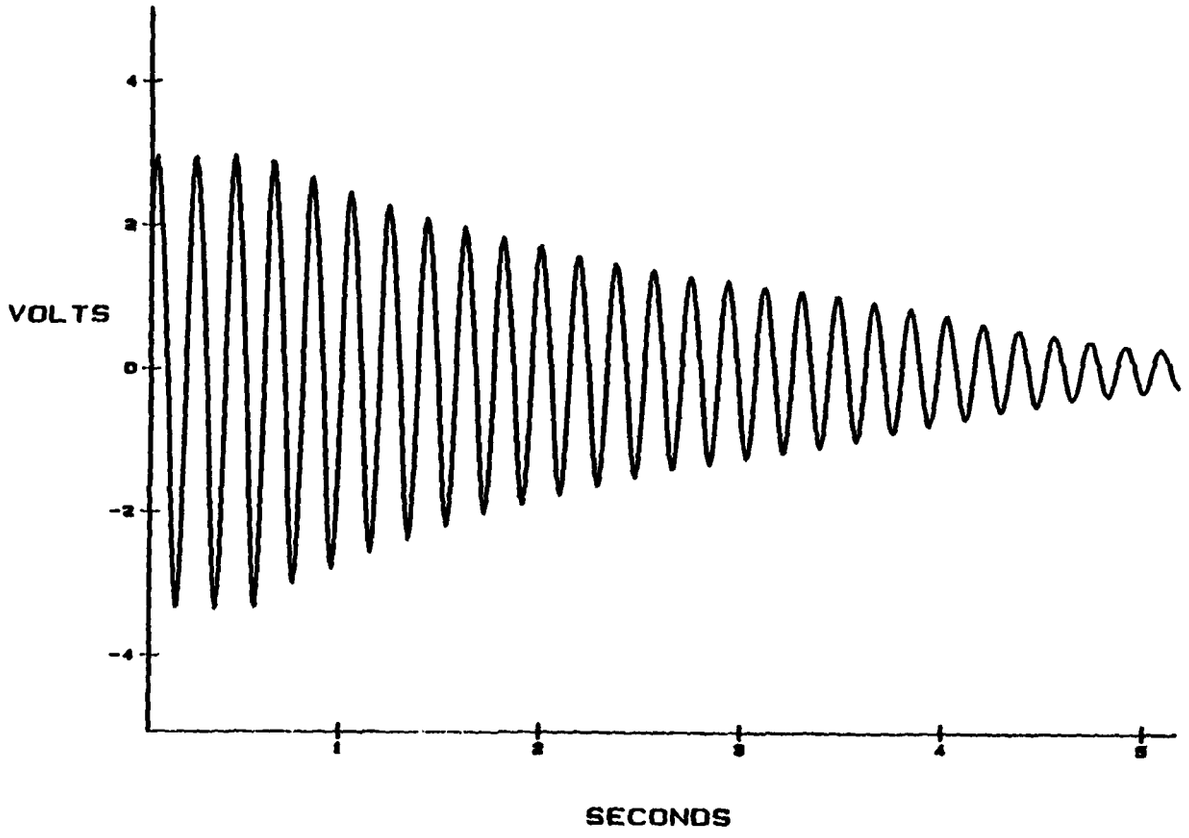

FIGURE 28. A plot of free decaying (0,1) mode surface-water-wave.

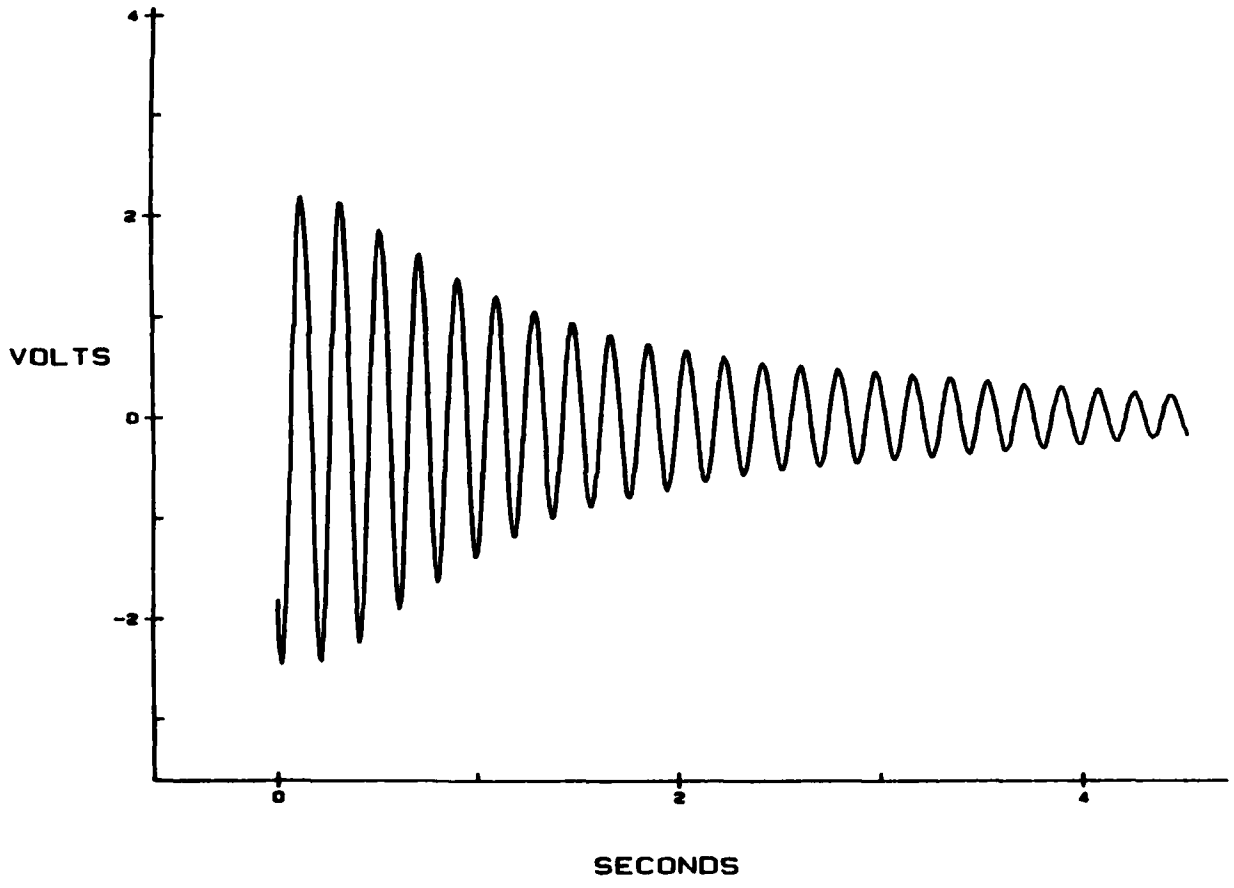

FIGURE 2 9 A plot of the free decaying soliton.

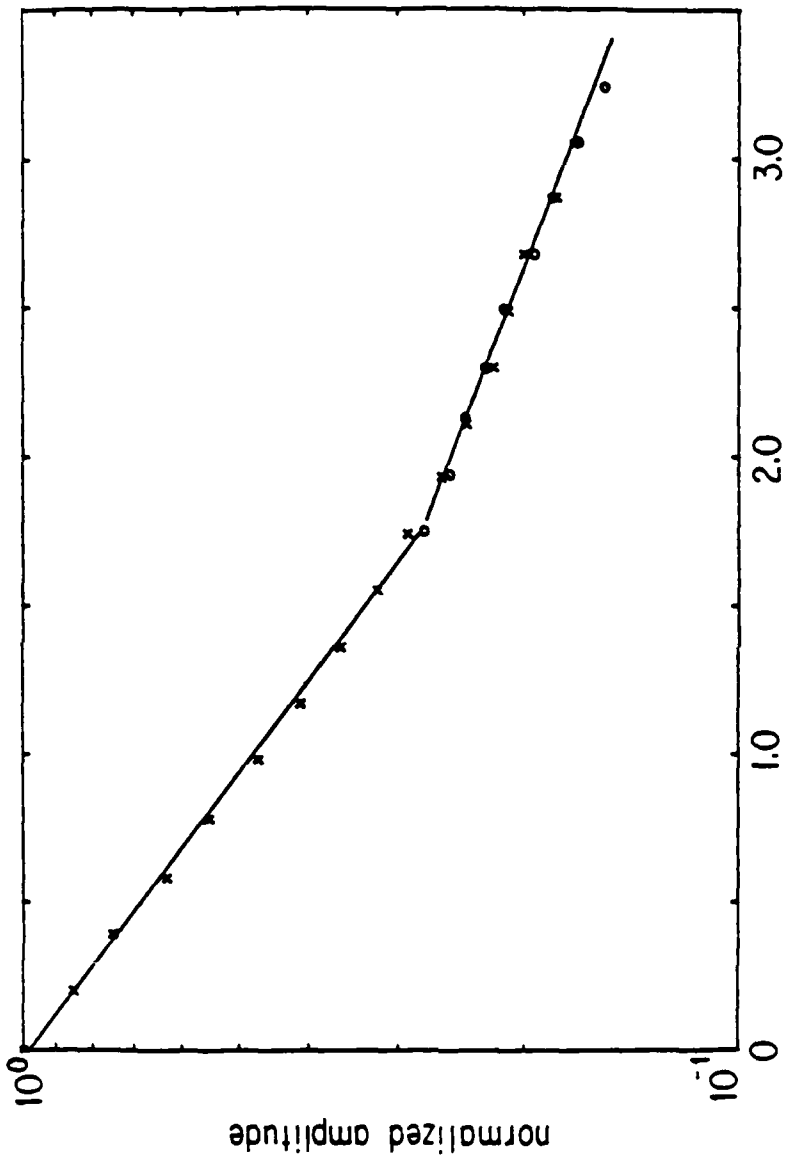

FIGURE 30. The amplitude of the same decaying (0,1) mode wave and soliton as Figs. 28 and 29. The circles are amplitudes of the (0,1) mode, and the points are that of the soliton.

CHAPTER VI

CONCLUSION

''The laws of physics
should be simple.''
A. Einstein[22]

A. SUMMARY

The experimental discovery of a unique nonpropagating hydrodynamic soliton whose excitation is that of a transverse surface-wave in a channel is reported. Like the polaron in solids, its energy is highly localized through a self-trapping effect. The profile of the soliton can be decribed by a hyperbolic secant function and the self-trapping occurs because the cutoff frequency for the transverse mode is a decreasing function of the wave amplitude. Accordingly the appropriate frequency for generation of the peak energy at the center of the soliton is below the cutoff frequency at the evanescent wings and above the amplitude dependent cutoff frequency at the peak. Measurements also show that this self-trapping behavior is absent when the liquid depth falls below a certain value, which is in

reasonable agreement with the theory[2],[3].

The interactions between solitons are also observed. Solitons with the same polarity attract each other, while the force between solitons with opposite polarity is repulsive. The breather-like internal oscillation of an in-phase soliton pair is seen to be very stable.

The free decay rate of the soliton is measured, and the measurements show that solitons initially decay faster than the corresponding transverse mode but have the same rate in the terminal decay.

B. FURTHER EXPERIMENTS AND THEORETICAL INVESTIGATIONS

As discussed earlier that the two essential conditions to create the nonpropagating soliton are:

a, The system must be dispersive enough to prohibit higher harmonic generation.

b, The cutoff frequency for propagating a transverse wave must decrease as the amplitude of wave increases.

It might be possible to find a dispersive system with higher dimensions which has a highly localized finite amplitude disturbance existing at a frequency less than the cutoff frequency of propagation in the surrounding medium. Thus the

disturbance cannot escape but exponentially decays into the surrounding region forming the soliton. One possible candidate might be the flexure mode in thin plates.

Another possibility is to look for the nonpropagating soliton in an acoustic, optical, or even biological waveguide-like system. Of couse the first thing to check is to see if the system has the properties which satisfy the above-mentioned conditions.

There are as yet no theoretical explanations of the breather-like oscillations of the in-phase soliton pair and the initial free decay rate of the soliton.

APPENDIX A

J. SCOTT RUSSEL'S REPORT ON HIS DISCOVERY

J. Scott Russel's Report on Waves at the British Association for the Advancement of Science was first published in 1845[5]. The following paragraph is the most fascinating part of the report of his great disvovery:

''I believe I shall best introduce this phenomenon by describing the circumstances of my own first acquaintance with it. I was observing the motion of a boat which was rapidly drawn along a narrow channel by a pair of horses, when the boat suddenly stopped - not so the mass of water in the channel which it had put in motion; it accumulated round the prow of the vessel in a state of violent agitation, then suddenly leaving it behind, rolled forward with great vilocity, assuming the form of a large solitary elevation, a rounded, smooth and well-defined heap of water, which continued its course along the channel apparently without change of form or diminution of speed. I followed it on horseback, and overtook it still rolling on at a rate of some eight or nine miles an hour, preserving its original figure some thirty feet long and a foot and a half in height. Its height

gradually diminished, and after a chase of one or two miles I lost it in the windings of the channel. Such, in the month of August 1834, was my first chance interview with that singular and beautiful phenomenon which I have called the Wave of Translation....''

APPENDIX B

KdV TYPE SOLITONS

In 1895 Korteweg and de Vries included both dispersion and nonlinearity, and derived the so-called KdV equation. There are different versions of derivation for the equation. The one, introduced as follows, is worked out by M. Olsen, H. smith and A. C. Scott in 1984[23].

For an incompressible, irrotational and inviscid fluid in a water tank, the velocity potential (Fig. 3), ϕ, satisfies the Laplace equation:

$$\nabla^2 \phi = 0 \qquad \text{(B-1)}$$

Let us consider waves propagating in x direction in the water tank of depth of d. The displacement of the free surface is specified by the function $\zeta(x,t)$ defined by

$$z = \zeta(x,t). \qquad \text{(B-2)}$$

Boundary condition at the bottom of the tank is the velocity, v, must be zero in z direction:

$$(v_z)_{z=-d} = (\delta\phi/\delta z)_{z=-d} = 0 \qquad \text{(B-3)}$$

At the free surface the boundary equations are specified the following two equatioins:

$$\delta\phi/\delta z - \delta\phi/\delta x \cdot \delta\zeta/x - \delta\zeta/\delta t = 0 \qquad \text{(B-4)}$$

$$\delta\phi/\delta t + \frac{1}{2}(\nabla\phi)^2 + g\zeta = 0 \qquad \text{(B-5)}$$

where the first one is the kinematic boundary equation and the second is Bennoulli's equation.

Let us express a solution of Eq. (B-1) satisfying the boundary conditions of Eq. (B-3) as a wave packet:

$$\phi = \frac{1}{2\pi}\int_{-\infty}^{\infty} dk \cosh k(d+z)\exp(ikx)g(k,t) \qquad \text{(B-6)}$$

where the weight function g(k,t) has its fourier transform f(x,t) given by

$$f(x,t) = \frac{1}{2\pi}\int_{-\infty}^{\infty} dk \exp(ikx)g(k,t) \qquad \text{(B-7)}$$

equal to the value of ϕ at the bottom of the tank, $z = -d$. We perform a simultaneous expansion for $z = \zeta(x,t)$ of Eq. (B-6) in terms of $\alpha = \zeta_{max}/d$ and $\beta = (d/\Lambda)^2 = O(\alpha)$, where Λ is the characteristic length of the soliton, and get that

$$\phi \simeq f(x,t) - \frac{1}{2}(d + \zeta)^2 f_{xx} \tag{B-8}$$

and

$$\phi_z \simeq -(d + \zeta) f_{xx} + \frac{1}{6}(d + \zeta)^3 f_{xxxx} \tag{B-9}$$

Thus Eq. (B-5) becomes

$$\zeta_t + [(d+\zeta) f_x]_x - \frac{1}{6} d^3 f_{xxxx} = 0 \tag{B-10}$$

by keeping terms to $\alpha = \zeta_{max}/d$ and $\beta = (d/\Lambda)^2 = O(\alpha)$ in our expansion, while Bernoulli's equation is

$$f_t + g\zeta - \frac{1}{2} d^2 f_{xxt} + \frac{1}{2}(f_x)^2 = 0 \tag{B-11}$$

From Eq. (B-10) and Eq. (B-11) the resulting linear dispersion relation for propagating plane wave becomes

$$\omega^2 \simeq c_o^2 k^2 (1 - \frac{1}{3} k^2 d^2) \tag{B-12}$$

where $c_o^2 = gd$.

If the function $\Sigma = f_x$ and the dimensionless valuables $x^* = \frac{x}{\Lambda}$, $t^* = \frac{t}{\Lambda}c_o$, $\zeta^* = \frac{\zeta}{\zeta_{max}}$ and $\omega^* = (\omega c_o)/(g\zeta_{max})$ are introduced, Eq. (B-11) and Eq. (B-12) can be rewritten as follows (dropping the stars):

$$\zeta_t + [(1+\alpha\zeta)\Sigma]_x - \frac{1}{6}\beta\Sigma_{xxx} = 0 \qquad \text{(B-13)}$$

$$\Sigma_t + \zeta_x - \frac{1}{2}\beta\Sigma_{xxt} + \alpha\Sigma\Sigma_x = 0. \qquad \text{(B-14)}$$

In order to determine an equation for ζ, valid to first order in α and β, we write $\Sigma = \zeta + \alpha A + \beta B$ and insert in Eqs.(B-13) and (B-14). The two equations become consistant if $A = -\frac{1}{4}\zeta^2$ and $B = \frac{1}{3}\zeta_{xx}$, and yield the KdV equation:

$$\zeta_t + \zeta_x + \frac{2}{3}\alpha\zeta\zeta_x + \frac{1}{6}\beta\zeta_{xxx} = 0. \qquad \text{(B-15)}$$

With the time and space variables restored this equation becomes the KdV equation in its usual form:

$$\zeta_t + c_o\zeta_x + \frac{3}{2}(c_o/d)\zeta\zeta_x + \frac{1}{6}d^2c_o\zeta_{xxx} = 0. \qquad \text{(B-16)}$$

It is convenient to nondimensionalize Eq. (B-16) in to a reference frame moving with the basic wave speed c_o by introducing the following variables:

$$\xi = (x-c_o t)/\Lambda,\ \tau = \frac{1}{6}\left(\frac{d}{\Lambda}\right)^2 (c_o t/\Lambda),\ \eta = \zeta/\zeta_{max}. \qquad \text{(B-17)}$$

The end result is

$$\eta_\tau + 6\eta\eta_\xi + \eta_{\xi\xi\xi} = 0. \qquad \text{(B-18)}$$

The soliton solution of Eq. (B-18) is

$$\eta = \zeta_{max}\,\mathrm{sech}^2\left[(\zeta_{max}/2)^{\frac{1}{2}}(\xi - 2\zeta_{max}\tau)\right] \qquad \text{(B-19)}$$

Korteweg and de Vries derived a somewhat more general equivalent of Eq. (B-16), in which they included a surface tension μ, such that coefficient d^2 in Eq. (B-16) is replaced by $L[1-(\frac{3\mu}{\rho g})^{\frac{1}{2}}/d]$. If $d_1 < (\frac{3\mu}{\rho g})^{\frac{1}{2}}$ (0.5 cm for water), Λ must be replaced by $|\Lambda[1-(\frac{3\mu}{\rho g})^{\frac{1}{2}}/d]|$, and Eq. (B-18) becomes:

$$\eta_\tau - 6\eta\eta_\xi + \eta_{\xi\xi\xi} = 0. \qquad \text{(B-20)}$$

Now the solution for this equation is a solitary wave of depression rather than elevation.

From Eq. (B-19) we notice that the velocity of the soliton is related to its amplitude in such a way that the soliton would

no longer exist as the velocity vanishes.

Figure 31 shows the KdV soliton observed by M. Olsen, et al[23].

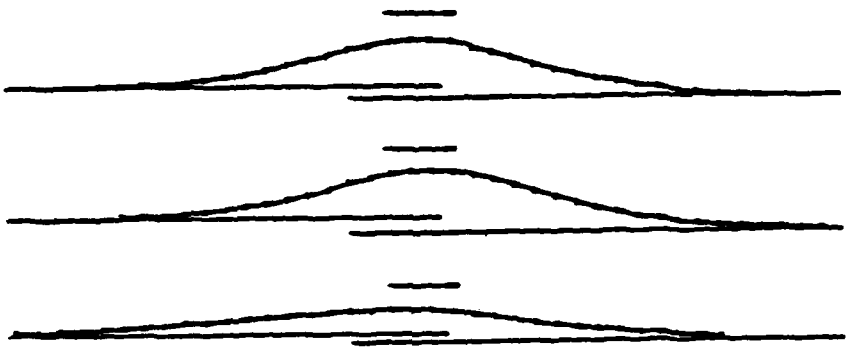

FIGURE 31. KdV type solitons observed by M. Olsen et al. Three different single waves going right. The solid curves are are experimental, the dots obtained from theory.

APPENDIX C

F.P.U. RECURRENCE

After world war II, Fermi became interested in the development and potentialities of the electronic computer. The first physical problem he decided to try is a problem for heuristic work. An one dimensional dynamic system of 64 particles with fixed boundary condition and nonlinear coupling between neast neighbors was studied on the Los Alamos computer Maniac I. The nonlinear terms considered are quadratic, cubic and broken linear types. The results are analyzed into fourier components and plotted out as a function of time. The original motivation was to observe the rates of thermalization. The results of the calculations were quite surprising; the time evolution of energy shows very little tendency toward equipartition of energy among the degrees of freedom.

Fig. 32 is a plot of the energy of the system versus time. The nonlinear coupling force here is quadratic. The initial position of the 64 particles string is a pure sine wave (the first mode). At beginning, the gradual energy flow from the first to the second and the third etc. was observed. Later on,

however, this gradual sharing of energy among successive modes ceases. Instead, it is one or the other mode that predominates. It is only the first few modes which exchange energy among themselves. Finally mode I comes back to within few persent of the initial value. This kind recurrence occurs to the cubic and broken linear coupling too. In 1970 M. Toda proved that this kind phenomenon can be approximately represented by the soliton solution of the so-called Toda lattice[24].

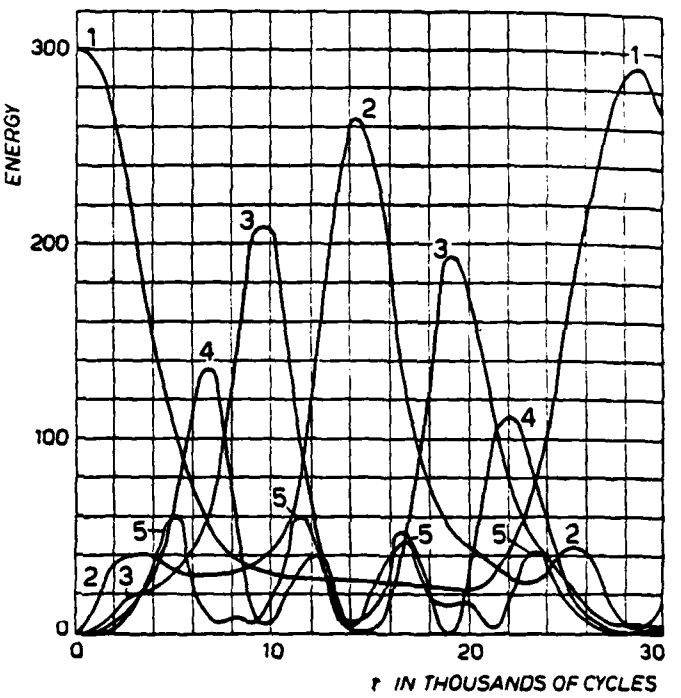

FIGURE 3 2 F.P.U. recurrence.

APPENDIX D

ENVELOPE SOLITONS

It was theoretically discovered by Lighthill[25] in 1965 that weakly nonlinear ($k\zeta_{max} = \varepsilon << 1$, k is wave number, $_{max}$ is the characteristic amplitude of the disturbance) deep-water ($kd >> 1$, d is the depth of water) wavetrain are unstable to modulation pertubations. In 1968 Zakharov[11] found that this modulation instability leads to the fact that the time evolution of weakly nonlinear deep-water wave obeys the nonlinear Schrodinger equation:

$$i\frac{\partial A}{\partial \tau} + \Lambda \partial^2 A/\partial \eta^2 = \nu |A^2| A \qquad \text{(D-1)}$$

where $\eta = \varepsilon k(\underline{x} - c_g t)$, $\tau = \varepsilon^2 (gk)^{\frac{1}{2}} t$, $c_g = \frac{\partial \omega}{\partial k}$,
$\Lambda = k^2/[2(gk)^{\frac{1}{2}}] \cdot \partial c_g/\partial \omega$, $\nu = \frac{15}{4}(\frac{k}{g})^{\frac{1}{2}} - 2gh/[k(kh)^{\frac{1}{2}}(gh - c_g^2)]$
and the free surface of water is

$$z = Re([\varepsilon i(kh)^{\frac{1}{2}} A/k^2] \exp[i(kx - \omega t]. \qquad \text{(D-2)}$$

In 1971 Zakharov and Shabat[26] solved NLS exactly by using the inverse scattering technique developed by Gardner et al[27].

The soliton solution of Eq. (D-2) is

$$A = a\left|\frac{2\Lambda}{\nu}\right|^{\frac{1}{2}} \operatorname{sech}[a(\eta - 2b\tau]\exp[ib\eta + i\Lambda(a^2-b^2)\tau] \qquad (D-3)$$

The solution shows that the disturbance, which is moving with group velocity c_g, is a localized wave packet with a fast oscillation of carrier frequency ω and an envelope specified by hyperbolic secant function. So it is known as the envelope soliton.

This theoretical prediction was verified by Yuen and Lake's experiments[12] in 1975. They use a 0.915 m × 0.914 m × 12.9 m water tank with a wavemaker at one end and a wave-absorbing beach at the other. The wavemaker is a hinged paddle activated by a hydraulic cylider. The time evolution of each initial wave was measured by capacitance wave amplitude gauges, which were put at 1.53, 3.05, 4.58, 6.10, 7.63 and 9.15 m in downstream of the wavemaker. Experimental results show that any initial wave packet, other than the soliton envelope described by Eq. (D-3), eventually evolves into a number of envelope solitons . Measurements also show solitons survive from the interaction of two envelope solitons (Figs. 33 and 34).

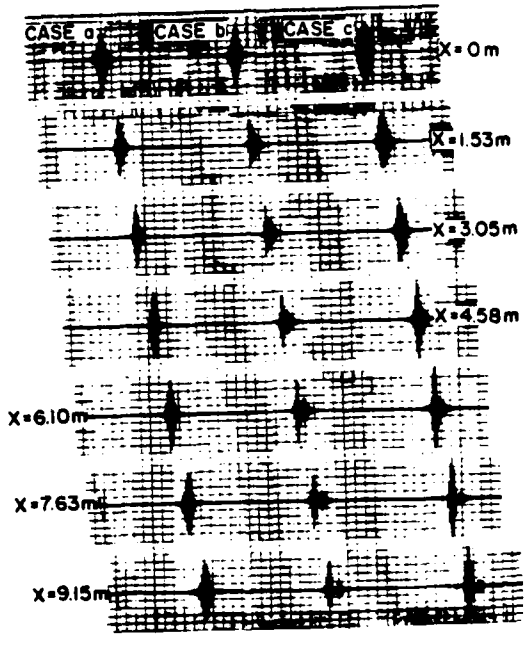

FIGURE 3 3 The initial pulses disintegrate into solitons. Case a, initial pulse with soliton profile. Case b, initial pulse with sech profile and amplitude twice that for soliton profile, amplitude scale of traces reduced by factor of 2.5 compared with case a and c. Case c, initial pulse with sine profile.

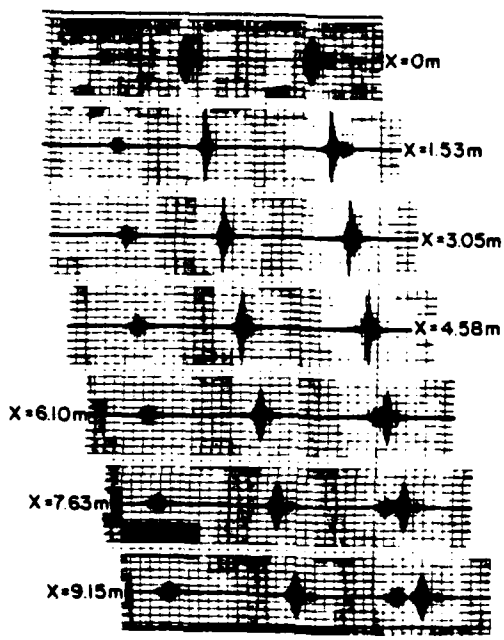

FIGURE 34 The interaction of envelope solitons. Left-hand trace: first pulse alone. Center trace: second pulse alone. Right-hand trace: the second one overtakes and passes through the first one.

AD-A155 569 DISCOVERY OF A NONPROPAGATING HYDRODYNAMIC SOLITON(U) 2/2
CALIFORNIA UNIV LOS ANGELES DEPT OF PHYSICS J R WU
JUN 85 TR-43

UNCLASSIFIED F/G 20/4 NL

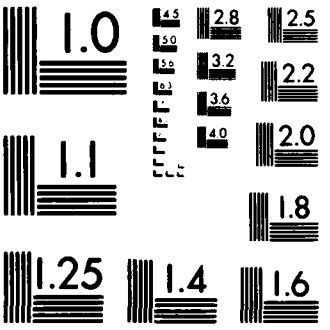

APPENDIX E

THE THEORY OF NONPROPAGATING SOLITONS

The theory of nonpropagating solitons were worked out by Miles[2], and by Larraza and Putterman[3] independently. Larraza and Putterman's approach neglects friction and drive, while Miles's approach includes dissipation as well as parametric drive, essentially identical results were achieved. This fact implies that neither dissipation nor parametric drive are central to our problem. For the sake of simplicity only the first approach is introduced as *follows*.

For an incompressible inviscid and irrotational fluid in a gravitational field, if surface tension effects are neglected the velocity potential, ϕ, satisfies Laplace's equation.

$$\nabla^2 \phi = 0. \qquad \text{(E-1)}$$

For the problem we want to solve (Fig. 3) the following boundary condition should be satisfied:

$$\phi_z = 0, \text{ at } z = -d, \qquad \text{(E-2)}$$

$$\phi_y = 0, \text{ at } y = 0, W. \tag{E-3}$$

At the free surface $z = \zeta(x,y,t)$ the boundary conditions are specified by two equations. One is so-called kinematic boundary condition, which is due to the fact that wave motion becomes stationary when it is observed in a reference frame moving with it. Consequently

$$d/dt[z-\zeta(x,y,t)] = 0 \tag{E-4}$$

or

$$\zeta_t+\phi_x\zeta_x+\phi_y\zeta_y = \phi_z, \text{ at } z = \zeta(x,y,t).$$

The other is the dynamic boundary condition which is specified by Bernoulli's equation:

$$\phi_t+g\zeta+1/2(\nabla\phi)^2 = 0, \text{ at } z = \zeta(x,y,t). \tag{E-5}$$

If the surface displacement $\zeta(x,y,t)$ is eliminated in favor of the velocity potential, ϕ, the following equation for ϕ valid up to terms that are cubic in derivatives of ϕ can be derived:

$$\phi_{tt}+g\phi_z = -\{(\nabla\phi)^2{}_t-[(\phi_z+\phi_{tt}/g)\phi_t]_z\} \qquad \text{(E-6)}$$
$$-1/2\{(\nabla\phi)^2{}_x\phi_x+(\nabla\phi)^2{}_y\phi_y+(\nabla\phi^2)_z\phi_z$$
$$-2/g[(\nabla\phi)^2{}_t\phi_t]_z-(\phi_z+\phi_{tt}/g)_z[(\nabla\phi)^2$$
$$-2/g(\phi_t{}^2)_z]\}+O(\varepsilon^4), \text{ at } z = 0.$$

Up to terms that are quadratic in gradients of ϕ, Eq. (E-6) can be rewritten as

$$g\zeta = -\phi_t+1/2[1/g(\phi_t)^2{}_z-(\nabla\phi)^2] \text{ at } z = 0. \qquad \text{(E-7)}$$

Considering the weakly nonlinear problem of a disturbance with a high frequency of motion ω in y-direction modulated by an envelope $\zeta_1(x,t)$ in x-direction and satisfying the following multiple-scale requirements:

$$k\zeta_{max} = \varepsilon << 1, \qquad \text{(E-8)}$$

$$(d\log\zeta/dx)/(d\log\zeta/dy) = O(\varepsilon), \qquad \text{(E-9)}$$

$$\omega_1{}^2/\omega^2-1 = O(\varepsilon^2), \qquad \text{(E-10)}$$

$$[1/(\omega\zeta_1)\cdot\partial\zeta_1]/\partial t = O(\varepsilon^2), \qquad \text{(E-11)}$$

where

$$\omega_1^2 = gkT,\ T = \tanh(kd),\ k = \pi/W. \qquad \text{(E-12)}$$

The solution of Laplace's equation specified by the boundary conditions Eqs. (E-2) and (E-3) is given by

$$\begin{aligned}\phi = {} & (\phi_1(x,t)[\cosh k(z+d)/\cosh kd]\cdot\cos ky\cdot\exp(i\omega t)+c.c.) \qquad \text{(E-13)}\\ & +[\phi_0^{(2)}(x,t)\exp(2i\omega t)+c.c.]+[\cosh 2k(z+d)/\cosh 2kd]\cdot\cos 2ky\\ & \cdot\{[\phi_2(x,t)\exp(2i\omega t)+c.c.]+\phi_2^{(0)}(x,t)\}+\{[-1/(2k)]\cdot\partial^2\phi_1/\partial x^2\\ & \cdot(\cos ky/\cosh kd)\cdot\exp(i\omega t)[z\sinh k(z+d)-d\exp(-k(z+d))]+c.c.\}\\ & +\phi_0[x+i(z+d),t]+\phi_0[x-i(z+d),t]+O(\varepsilon^4).\end{aligned}$$

Substituting Eq. (E-13) into Eq. (E-7) and equating to zero coefficients of the same $\cos(mky)\exp(ni\omega t)$ dependence, the following solutions of different orders can be determined

$$\omega_0^2 = kgT \quad \text{(valid to } O(\varepsilon)) \qquad \text{(E-14)}$$

$$\phi_2 = [(-3ik^2\phi_1^2)/(8\omega T^2)](1-T^4) \quad \text{(valid to } O(\varepsilon^2)) \qquad \text{(E-15)}$$

$$\phi_0^{(2)} = [ik^2/(8\omega)]\phi_1^2(1+3T^2) \qquad \text{(E-16)}$$

(valid to $O(\varepsilon^2)$)

$$\phi_2^{(0)} = 0 \quad \text{(valid to } O(\varepsilon^2)) \qquad \text{(E-17)}$$

and

$$2i\omega\partial\phi_1/\partial t - c^2\partial^2\phi_1/\partial x^2 + (\omega_1^2 - \omega^2)\phi_1 - Ak^4\phi_1^2\phi_1 = 0 \quad \text{(valid to } O(\varepsilon^3)\text{)} \tag{E-18}$$

where

$$c^2 = \frac{g}{2k}[T + kd(1-T^2)] \tag{E-19}$$

and

$$A = 1/8(6T^4 - 5T^2 + 16 - 9T^{-2}). \tag{E-20}$$

If the surface tension effects are included, as worked out by Miles[2], Eqs.(E-19) and (E-20) should respectively modified as

$$\omega_0^2 = (kg + \frac{\mu}{\rho}k^3)T \tag{E-21}$$

and

$$A = \frac{1}{2}[1 + (1-T^2)^2 + \frac{1}{2}(1+4\mu^*)^{-1}(1+T^2)^2 - \frac{1}{4}(T^2 - 4\mu^*)^{-1}(3-T^2)^2] \tag{E-22}$$

where μ is surface tension, and $\mu^* = \mu(\frac{\pi}{W})^2/(\rho g)$.

We introduce amplitude dependent cutoff frequency, $\omega_0(\zeta)$, which is given by

$$\omega_0^2(\zeta) = \omega_0^2 - Ak^4\phi_1^2 \tag{E-23}$$

or

$$v_e(\zeta_{max}) \simeq v_e(1-Ag^2\zeta_{max}^2/(128W^4v_e^4). \qquad \text{(E-24)}$$

Under the condition that A>0, which means that d>1.022/k from Eq.(E-20), $\omega_e(\zeta)<\omega_e$. As $\omega_e<\omega<\omega_e(\zeta)$, Eq.(E-18) possesses a soliton solution of the form

$$\phi_1 = [2(\omega_e^2-\omega^2)/(Ak^4)]^{\frac{1}{2}}\text{sech}[(\omega_e^2-\omega^2)x/c^2] \qquad \text{(E-25)}$$

The surface displacement, $\zeta(x,y,t)$, can be calculated from Eq.(E-7) as

$$\begin{aligned}\zeta(x,y,t) = \frac{1}{g}\{&[-i\omega\phi_1\exp(i\omega t)\cos ky+c.c.] \qquad \text{(E-26)}\\ &+[\frac{1}{2}k^2|\phi_1|^2(T^2+1)\cos 2ky + \frac{1}{2}k^2|\phi_1|^2(T^2-1)\\ &-\frac{1}{4}k^2\phi_1^2\,(\frac{3}{T^2}-1)\exp(2i\omega t)\cos 2ky+c.c.]\}\end{aligned}$$

In summary, the solution has the following features:

(1) the shape of the modulation is given by hyperbolic secant function.

(2) the soliton is stationary along x-direction.

(3) the amplitude and width of the soliton are determined by the liguid depth, d, and the frequency of the excitation for a particular trough.

These characteristics qualitatively match our experimental observation.

REFERENCES

1. J. Wu, R. Keolian, and I. Rudnick, Phys. Rev. Lett. 52, 1421(1984).
2. J. W. Miles, J. Fluid Mech. 148, 450(1984).
3. A. Larraza and S. Putterman, J. Fluid Mech. 148, 443 (1984), and Phys. Lett. 103A, 15(1984). M. Cabot, Ph. D. thesis, UCLA(1983).
4. T. D. Lee, Particle Physics and Introduction to Field Theory, 117(Harwood Academic Publishers, Chur, Switzland 1981).
5. J. Scott Russel, Report on Waves, Proc. Roy. Soc. Edinburgh, 319(1844).
6. Lord Rayleigh, Scientific Papers by Lord Rayleigh, Vol.I 38, 251(Dover, New York, 1964).
7. D. J. Korteweg and G. deVries, Phil. Mag.,39, 422(1895).
8. E. Segre, Collected Papers of Enrico Fermi, Vol.II, 978(University of Chicago Press, 1965).
9. N. J. Zabusky and M. D. Kruskal, Phys. Rev. Lett., 15, 240(1965).
10. A. C. Scott, F. Y. F. Chu and D. W. Mclaughlin,

Proc. IEEE, 61, 10(1973).

11. V. E. Zakharov, Zh. Prikl. Mekh. Tekh. Fiz. 2, 86(1968). Translated in J. Appl. Mech. Tech. Phys. 2,190(1968).

12. H. C. Yuen and B. M. Lake, Phys. Fluid, 18, 956(1975).

13. H. C. Yuen and B. M. Lake, Ann. Rev. Fluid Mech. 12, 303(1980).

14. H. Woolf, Some Strangeness in the Proportion, a centennial symposium to celebrate the achievements of Albert Einstein, 57(Addison-Wesley Publishing Co., Massachusetts, 1980).

15. P. Hagedorn, Nonlinear Oscillations, (Oxford Univ. Press, New York, 1981).

16. T. B. Benjamin and F. Ursell, Proc. Roy. Soc. A 225, 505(1954).

17. F. Ursell, Proc. Roy. Soc. A 214, 79(1952).

18. K. M. Case and W. C. Parkinson, J. Fluid Mech. 2, 172(1957).

19. G. H. Keulegan, J. Fluid Mech., 6, 33(1959).

20. W. G. Van Dorn, J. Fluid Mech., 24, 769(1966).

21. J. W. Miles, Proc. Roy. Soc. A297, 459(1967).

22. H. Woolf, Some Strangeness in the Proportion, a centennial sympasium to celebrate the achievements of Albert Einstein, 61(Addison-Wesley Publishing Co.

Massachusetts,1980).

23. M. Olsen, H. Smith and A. C. Scott, Am. J. Phys. 52(9), 826(1984).

24. M. Toda, Progr. Theo. Phys. Suppl. 45, 174(1970).

25. M. J. Lighthill, J. Inst. Math. Appl. 1, 269(1965).

26. V. E. Zakharov and A. B. Shabat, Sov. Phys. JETP 34, 62(1972).

27. C. S. Gardener, J. M. Greene, M. D. Kruskal and R. M. Miura, Phys. Rev. Lett.19, 1095(1967).

END

FILMED

8-85

DTIC